Imperial College London

MSc Dissertation

Imperial College London

Department of Physics

Numerical Calabi-Yau Metrics and Machine Learning

Author:

Wong Kwok Yiu, Sunny

Supervisor:

Prof. Toby Wiseman

Submitted in partial fulfilment of the requirements for the degree of Master of Science of Imperial College London

September 22, 2023

Abstract

This dissertation aims to review the current methods of obtaining numerical Calabi-Yau metrics. We start by introducing complex manifolds and study the geometry and structure of a Kähler manifold. We review the celebrated theorem of Yau and motivate the study of Calabi-Yau manifolds in physics. We then discuss the success and limitations of the two mainstream algorithms which solve for a numerical Calabi-Yau metric, namely Donaldson's algorithm and the Energy functional approach. With the recent advancements in the field of machine learning, physicists and mathematicians apply neural networks to approximate the Calabi-Yau metrics with greater efficiency but sometimes less accuracy compared to traditional numerical methods. At the end of this dissertation, we will discuss if machine learning is necessary in the study of numerical Calabi-Yau metrics, and discuss how this rapidly evolving technology can help string theorists in their computations.

Acknowledgements

I would like to express my gratitude to my supervisor, Professor Toby Wiseman, for our valuable discussions and guidance throughout the summer. I would also like to thank my fellow QFFF coursemates, especially Albert, Andres and Matthew, for making this academic year fantastic. Lastly, I would like to thank my friends, family and my partner, Odelia, for their constant support. Without them, it would not have been possible to complete my QFFF studies.

Contents

1 Introduction

String theory is by far one of the most promising candidates in unifying quantum theory with general relativity. It posits that the fundamental building blocks of the universe is an object with two degrees of freedom, called strings. The first formulation of a string theory is called the Bosonic string theory which is only consistent in a 26-dimensional space. However, it has no fermionic content as suggested by the name of the theory and allows the existence of tachyons. Later developments in string theory led physicists to formulate the superstring theory which solves the previously mentioned problems. Superstring theory is formulated in a 10-dimensional space, and we have currently 5 different types of them, that is type I, type IIA, type IIB, heterotic $E_8 \times E_8$ and the $SO(32)$ superstring theory.

One of the methods for obtaining a Standard Model like physics from a string theory is by doing a superstring compactification. The goal of compactification is to obtain a 4-dimensional low-energy effective field theory (EFT), which describes our universe, from the 10-dimensional string theory. This can be done by, first, assuming the 10-dimensional space is a product space of a 4-dimensional manifold (i.e. where we live in, Minkowski) with a 6-dimensional compact space, $\mathcal{M}$, called the internal space. Secondly, to allow the theory to describe our universe, we must compactify $\mathcal{M}$ such that it is too small to be observed. In addition, we demand the metric on $\mathcal{M}$ to satisfy Einstein's field equations, which equates the Ricci tensor of $\mathcal{M}$ to the energy tensor describing the vacuum energy. A natural postulate would be setting the vacuum energy to zero, implying the metric on $\mathcal{M}$ is Ricci-flat.

Ricci-flatness condition is not enough to reproduce for a Standard Model like physics in the low-energy EFT. Properties of the internal space geometry, for instance, its moduli spaces, restrict how the low-energy EFT behaves. To achieve the $SU(3) \times$

$SU(2) \times U(1)$ Standard Model gauge group, we require $\mathcal{M}$ to carry a holomorphic vector bundle of rank 3,4 or 5, with a connection that solves the Yang-Mills equations [1]. The first attempt at obtaining Standard Model like physics from a superstring theory, explicitly from the heterotic $E_8 \times E_8$ superstrings, was made by [2] in 1985. They have provided us with the necessary conditions for the right internal space and continue to serve as an example of how superstring compactification is done.

Remarkably, the simplest candidates for the internal space are called the Calabi-Yau manifolds. The significance of Calabi-Yau manifolds is that they admit a unique Ricci-flat metric and preserve some of the supersymmetry from the superstring under compactification. The story of Calabi-Yau manifolds originates from the 1950s when Calabi gave his well-known conjecture [3], that is there exists a unique Ricci-flat metric in every Kähler class on a Kähler manifold with vanishing first Chern class. Calabi managed to prove the uniqueness of such a metric but did not prove its existence. Later in 1978, Yau proved Calabi's conjecture [4] through the study of complex Monge-Ampeŕe equation. However, Yau's celebrated theorem did not tell us how to get the explicit expression of such a unique Ricci-flat Kähler metric.

Despite not knowing the explicit analytic expression of the Calabi-Yau metrics, tools from differential geometry and algebraic geometry still allow us to probe the topology of the manifold and study how it constrains our low-energy EFT.

An obvious condition to check is whether the Calabi-Yau manifold gives rise to the three generations of quarks and leptons. This restricts its Euler characteristic to have $\chi = \pm 6$. Early work in finding such Calabi-Yaus includes [5, 6]. So far, half a billion Calabi-Yau threefolds have been constructed and classified in the Kreuzer-Skarke (KS) data set, accessible via link [7]. Any of these Calabi-Yau threefold with $\chi = \pm 6$ are potentially our compactification space, and each of them corresponds to a different universe with different particle spectrums and particle interactions. In literature, this vast amount of Calabi-Yaus forms the "Calabi-Yau Landscape" [8].

Having matched with the desired particle content and interactions, we would need to compute physical observables, such as coupling strength and masses of the fermions. However, it would require the knowledge of the Calabi-Yau metrics. Unfortunately, up till today, there is no known explicit analytic expression for the Calabi-Yau metric on Calabi-Yau threefolds. This motivates the study of numerical Calabi-Yau metrics, gathering efforts from both mathematicians and string theorists.

Headrick and Wiseman [9] were the first ones to compute the Calabi-Yau metric numerically on the K3 surface, a Calabi-Yau twofold. They introduced coordinate patches to discretize the Monge-Ampere equation on a lattice and developed a Gauss-Seidel-type relaxation algorithm to solve the equation. However, such a position-space method faces the clumsiness of coordinate patches and is limited by storage problems. It was found to be inefficient if it were to be applied to the Calabi-Yau threefold. Later, Donaldson [10] adopted the use of algebraic metrics, an idea advocated by Yau, which eliminates the need for coordinate patches.

Donaldson's algorithm starts by embedding a Calabi-Yau threefold X onto the ambient space $\mathbb{CP}^4$ as an algebraic variety. Then, it uses the sections of the holomorphic line bundle on X, which are some polynomials, to represent the Kähler potential on the ambient space. Metrics represented by such polynomials are called "algebraic". By iterating through a "T-map" k-times, the Kähler metric obtained from the Kähler potential is guaranteed to converge to a Ricci-flat metric in the limit of $k \to \infty$. A metric obtained through the T-map is called a balanced metric, and it is predicted to have an exponential convergence.

However, it was found that Donaldson's algorithm is inefficient for large k-values since the T-map involves integrating over X, which is a six-dimensional integral and thus is computationally challenging. In addition, metrics did not converge exponentially as predicted by the use of algebraic metrics. Nonetheless, most subsequent studies on the numerical Calabi-Yau metrics build up on Donaldson's algorithm

and were applied to study the hermitian Yang-Mills connection [11, 12, 13] and the eigenvalues and eigenfunctions of the scalar Laplace operator [14].

An alternate approach, which also implements algebraic metrics, is called the energy functional minimisation algorithm developed by Headrick and Nassar [15]. Instead of iterating through the T-map, they found a set of energy functionals which have a minimum that corresponds to a unique Ricci-flat metric on a Calabi-Yau. The authors referred them to the optimal metrics. The merit of this approach is that from a computational standpoint, minimising a non-linear function is always easier than integrating a non-linear function. Moreover, optimal metrics were shown to have significant improvement in resolution compared to that of the balanced metrics.

However, the major drawback is the algorithm's dependence on the symmetries of the Calabi-Yau. This is because symmetries on the Calabi-Yau were used to reduce the number of basis polynomials which in turn constrain the space of Kähler class it scans over. Therefore, with no symmetries, the space it scans over would be large and thus the algorithm would be inefficient. Unfortunately, most of the Calabi-Yaus of interest to string theory has little to no symmetries.

Both algorithm faces runtime and computer resources problems. Fortunately, numerous attempts were made to apply machine learning techniques to mitigate the aforementioned problems. It was shown that neural networks [16] are capable of approximating Calabi-Yau metrics with resolution on par with $k = 20$ balanced metrics, which was predicted to have a runtime of 35 years [17]. Moreover, the study of moduli dependence on the metric is made possible by the application of neural networks.

In this dissertation, chapter 2 gives a review of complex geometry and provides the necessary tools to understand Kähler manifolds and their topology. Chapter 3 gives an introduction to Calabi-Yau manifolds and studies some important properties which will be used in constructing numerical Calabi-Yau metrics. Chapter 4 gives

a review of both Donaldson's algorithm and the energy minimisation approach, followed by a brief discussion of their merits and limitations. The final chapter, chapter 5, gives an introduction to neural networks and explains how they approximate a Calabi-Yau metric. Through this dissertation, we hope to show the importance of Calabi-Yau manifolds in both mathematics and string theory and also show the potential of machine learning.

2 Complex Geometry

In essence, Calabi-Yau manifolds are compact Kähler manifolds with a vanishing first Chern class [4], which is Ricci-flat. To elaborate, complex manifolds are naturally equipped with an almost complex structure. Such an object defines a natural two-form on a Hermitian manifold, called the Hermitian two-form, or sometimes called the Kähler form. A Hermitian manifold is called Kälher if this natural two-form is closed. Surprisingly, Kähler manifolds have special geometric properties that lead to great simplifications. For instance, Kähler metrics can be represented by only a single function, namely the Kähler potential.[1] Finally, with Yau's theorem, we then learn that Kähler manifolds with vanishing first Chern class admit a Ricci-flat metric, and thus yields the definition of the Calabi-Yau manifold.

In this chapter, we will build up the necessary mathematical tools to understand the above paragraph and provide simple examples of how Calabi-Yaus can be constructed. Fundamental knowledge of differential geometry (on real manifolds), explicitly the chapters 2-7 (ch 3 optional) of [18], is assumed. The following chapters are based on [19, 20, 21, 22, 23, 24, 25, 18].

2.1 Complex Manifolds

Recall that a topological manifold is locally Hausdorff and is locally Euclidean. This is a necessary condition for us to introduce calculus onto the manifolds. For our purposes, we call topological manifolds as manifolds in this chapter. Loosely speaking, a m-dimensional real manifold is a Hausdorff topological space with a local homeomorphism. In addition, the manifold is provided with atlases and transition functions between coordinate patches are smooth.

[1] The Kähler potential holds a significant role in numerical Calabi-Yau metrics. See chapters 2.2.4 and 3 for elaboration.

Complex manifolds and real manifolds are defined similarly. The crucial difference between them is that transition functions are required to be holomorphic (analytic) on a complex manifold. We now define what holomorphic means.

Definition 2.1.1 *A complex function f, which can be expressed by two real-valued functions f_1 and f_2 (i.e. $f = f_1 + if_2$), is said to be holomorphic if it satisfies the Cauchy-Riemann equations,*

$$\frac{\partial f_1}{\partial x} = \frac{\partial f_2}{\partial y}, \qquad \frac{\partial f_1}{\partial y} = -\frac{\partial f_2}{\partial x} \tag{2.1}$$

where the complex coordinate is $z = x + iy$.

We can now define what a complex manifold is.

Definition 2.1.2 *A m-dimensional complex manifold $\mathcal{M}$:*

(i) *$\mathcal{M}$ is a Hausdorff topological space.*

(ii) *$\mathcal{M}$ is provided with 'atlases': a family of pairs $\{(U_i, \phi_i)\}$.*

(iii) *$\{U_i\}$ is a family of open sets which covers $\mathcal{M}$. ϕ_i is a homeomorphism from U_i onto an open subset U_i' of $\mathbb{C}^m$.*

(iv) *On the non-trivial overlapping chart region, $U_i \cap U_j \neq \emptyset$, the transition function $\psi_{ij} = \phi_i \circ \phi_j^{-1}$ from $\phi_j(U_i \cap U_j)$ to $\phi_i(U_i \cap U_j)$ is holomorphic.*

Within each coordinate patch, U_i, we choose local coordinates (complex coordinates in our case) z_i^μ $(\mu = 1, ..., m)$ such that our choice of coordinates can be related by the transition function on the overlapping region of two coordinate patches, i.e.

$$z_i^\mu = \psi_{ij}^\mu(z_j). \tag{2.2}$$

In addition, complex coordinates can always be expressed by two real coordinates, which allows us to treat m-dimensional complex manifolds as 2m-dimensional real manifolds. However, the converse does not always hold.

Example: Complex Projective Space $\mathbb{CP}^N$

One of the most straightforward methods of constructing Calabi-Yau manifolds is to construct them as a hypersurface embedded in the complex projective space $\mathbb{CP}^N$. The motivation for this will come clear in later chapters. Here, we will show that the $\mathbb{CP}^N$ is an N-dimensional complex manifold.

Definition 2.1.3 *Consider the space $\mathbb{C}^{N+1}\backslash\{0\}$, which contains complex coordinates $\{z^i\}$, $i = 1, 2, ..., N+1$, such that there is at least one z^i being non-zero. The complex projective space $\mathbb{CP}^N$ is defined as the space where we identify*

$$(z^1, z^2, ..., z^{N+1}) \sim \lambda(z^1, z^2, ..., z^{N+1}) \tag{2.3}$$

for any non-zero complex λ.

We can view this space as a set of undirected complex lines through the origin of $\mathbb{C}^{N+1}$. One often refers to the coordinates $\{z^i\}$ as the homogeneous coordinates defined in projective geometry. Now we examine if $\mathbb{CP}^N$ is a complex manifold.

We can construct (N+1) charts on the manifold, such that the i-th coordinate patch $U_{(i)}$ contains all the points on $\mathbb{CP}^N$ with $z^i \neq 0$. We now introduce the inhomogeneous coordinates on the i-th patch, that is

$$\zeta^\mu_{(i)} = \frac{z^\mu}{z^i}, \qquad \mu = 1, ..., N \text{ and } z^i \neq 0. \tag{2.4}$$

The chart homeomorphism $\phi_i : \mathbb{CP}^N \to \mathbb{C}^N$ gives us a map for $p \in \mathbb{CP}^N$,

$$p = (z^1, z^2, ..., z^{N+1}) \to (\zeta^1_{(i)}, \zeta^2_{(i)}, ..., \zeta^N_{(i)}). \tag{2.5}$$

On the non-trivial patch overlapping region, $U_{(i)} \cap U_{(j)}$, we have,

$$\zeta^\mu_{(i)} = \frac{z^\mu}{z^i} = \frac{z^\mu}{z^j}\frac{z^j}{z^i} = \frac{\zeta^\mu_{(j)}}{\zeta^i_{(j)}} \tag{2.6}$$

which is holomorphic (since neither z^i nor z^j is zero), and thus concludes that $\mathbb{CP}^N$ is a complex manifold. The significance of the complex projective space is that it is compact and Kähler, and thus its submanifolds are also compact. Kähler manifolds

will be introduced in later chapters, however, we will not show the compactness of $\mathbb{CP}^N$ here but we refer the readers to [26] for a proof.

An important theorem by Chow in algebraic geometry [27] states that all analytic submanifolds of $\mathbb{CP}^N$ can be realised as the zero locus of a finite number of polynomials of the homogeneous coordinates $\{z^i\}$. Such space is also referred to as an algebraic variety. An example of this is the Fermat quintic in $\mathbb{CP}^4$, defined as the zero locus of the polynomial,

$$P(z) = \sum_{\mu=0}^{4} (z^\mu)^5 = 0. \tag{2.7}$$

The Fermat quintic is a compact Calabi-Yau threefold which is studied intensively in the field of numerical metrics.

2.1.1 Almost Complex and Complex Structure

We have two types of coordinates on a local complex coordinate patch, that is the complex coordinate and its complex conjugate. On a m-dimensional complex manifold, we have a natural basis on its tangent space and the dual,

$$\{\frac{\partial}{\partial z^1}, \frac{\partial}{\partial z^2}, ..., \frac{\partial}{\partial z^m}; \frac{\partial}{\partial z^{\bar{1}}}, \frac{\partial}{\partial z^{\bar{2}}}, ..., \frac{\partial}{\partial z^{\bar{m}}}\}$$
$$\{dz^1, dz^2, ..., dz^m; dz^{\bar{1}}, dz^{\bar{2}}, ..., dz^{\bar{n}}\}$$

where $z^{\bar{\mu}}$ is the shorthand notation for the μ-th component of the complex conjugate of z. We now refer holomorphic and anti-holomorphic indices to μ and $\bar{\mu}$ respectively. The complex basis can be related to the real coordinate basis via

$$\frac{\partial}{\partial z^\mu} = \frac{1}{2}(\frac{\partial}{\partial x^\mu} - i\frac{\partial}{\partial y^\mu}), \quad \frac{\partial}{\partial z^{\bar{\mu}}} = \frac{1}{2}(\frac{\partial}{\partial x^\mu} + i\frac{\partial}{\partial y^\mu})$$
$$dz^\mu = dx^\mu + idy^\mu, \quad dz^{\bar{\mu}} = dx^\mu - idy^\mu$$

We know that any m-dimensional complex manifold $\mathcal{M}$ can always be treated as a 2m-dimensional real manifold $\mathcal{N}$. The interesting question to ask is when does the converse hold?

To tackle the question, one needs the notion of complex structure. Now write the complex indices as $\mu = 1, 2, ..., m$ and the real indices as $n = 1, 2, ..., 2m$.

Definition 2.1.4 *On a m-dimensional complex manifold $\mathcal{M}$ with local coordinates $\{z_i^\mu\}$ on the coordinate patch $U_{(i)}$, we can define a mixed tensor, called the almost complex structure $J_n{}^k$ via*

$$J = idz^\mu \otimes \frac{\partial}{\partial z^\mu} - idz^{\bar{\mu}} \otimes \frac{\partial}{\partial z^{\bar{\mu}}}. \tag{2.8}$$

The almost complex structure is a real tensor that squares to minus the identity,

$$J_n{}^k J_k{}^l = -\delta_n^l. \tag{2.9}$$

From equation (2.8), we have the tensor components in a complex basis

$$J_\mu{}^\nu = i\delta_\mu{}^\nu \,,\; J_{\bar{\mu}}{}^{\bar{\nu}} = -i\delta_{\bar{\mu}}{}^{\bar{\nu}} \,,\; J_{\bar{\mu}}{}^\nu = J_\mu{}^{\bar{\nu}} = 0. \tag{2.10}$$

Thus, one can express J as a matrix of form

$$J = \begin{pmatrix} i\mathbb{I}_{m\times m} & 0 \\ 0 & -i\mathbb{I}_{m\times m} \end{pmatrix} \tag{2.11}$$

where $\mathbb{I}_{m\times m}$ is the m-dimensional identity matrix. Going into the real basis (x^μ, y^μ) where $z^\mu = x^\mu + iy^\mu$, one can verify that equation (2.8) is equivalent to

$$J = dx^\mu \otimes \frac{\partial}{\partial y^\mu} - dy^\mu \otimes \frac{\partial}{\partial x^\mu}, \tag{2.12}$$

which implies J being real. This leads to the real matrix expression

$$J = \begin{pmatrix} 0 & \mathbb{I}_{m\times m} \\ -\mathbb{I}_{m\times m} & 0 \end{pmatrix}. \tag{2.13}$$

It is obvious that in either case the matrix squares to $-\mathbb{I}_{2m\times 2m}$. Taking J to act on a complex basis, we get the following useful properties

$$J(\frac{\partial}{\partial z^\mu}) = i\frac{\partial}{\partial z^\mu}, \qquad J(\frac{\partial}{\partial z^{\bar{\mu}}}) = -i\frac{\partial}{\partial z^{\bar{\mu}}}. \tag{2.14}$$

Thus, we can think of J as the multiplication of $\pm i$ as in complex analysis.

Using the almost complex structure tensor, we define two projection tensors

$$P_m{}^n = \frac{1}{2}(\delta_m{}^n - iJ_m{}^n), \quad Q_m{}^n = \frac{1}{2}(\delta_m{}^n + iJ_m{}^n) \tag{2.15}$$

which has the following properties

$$P^2 = P, \qquad Q^2 = Q, \qquad PQ = 0, \qquad P + Q = \mathbb{I}_{2m\times 2m}. \tag{2.16}$$

In a complex basis, one substitute (2.10) into (2.15) finds the only non-zero components of P and Q being $P_\mu{}^\nu = \delta_\mu{}^\nu$ and $Q_{\bar{\mu}}{}^{\bar{\nu}} = \delta_{\bar{\mu}}{}^{\bar{\nu}}$ respectively. This yields the matrix representation

$$P = \begin{pmatrix} \mathbb{I}_{m\times m} & 0 \\ 0 & 0 \end{pmatrix} \quad \text{and} \quad Q = \begin{pmatrix} 0 & 0 \\ 0 & \mathbb{I}_{m\times m} \end{pmatrix}. \tag{2.17}$$

It is immediately obvious that P acting on a tensor field $\mathcal{T}$ projects out the holomorphic components of $\mathcal{T}$, while Q projects out its anti-holomorphic components. Moreover, it implies that the tangent space is decomposable into a space of holomorphic vectors and a space of anti-holomorphic vectors.

Definition 2.1.5 *A real manifold equipped with an almost complex structure J is called an almost complex manifold.*

A complex manifold always admit a globally defined $J_n{}^k$ that squares to $-\mathbb{I}$. It prompts us to think if a real manifold that admits such a tensor is necessarily a complex manifold.

On a 2m-dimensional real manifold $\mathcal{N}$, consider the projection tensor acting on a coordinate differential, $A^n = P_k{}^n dx^k$. If $\mathcal{N}$ is also a complex manifold, then there exist local coordinates z^μ that allow us to write $A^n = A_\mu{}^n dz^\mu$, yielding

$$P_k{}^n dx^k = A_\mu{}^n dz^\mu. \tag{2.18}$$

Thus, for $\mathcal{N}$ to be a complex manifold, we have to ensure the existence of the complex coordinates z^μ and prove that different complex coordinates on overlapping coordinate patches are holomorphic functions of each other.

To examine if such complex coordinates exist, we need the Niejenhuis tensor.

Definition 2.1.6 *For two vector fields v,w, the Niejenhuis tensor of the almost complex structure J, N_J, is defined by*

$$N_J(v,w) = [v,w] + J[v,Jw] + J[Jv,w] - [Jv,Jw], \tag{2.19}$$

where $[\cdot,\cdot]$ denotes the Lie bracket of vector fields.

Locally, N_J has components $N^i_{jk} = J^l_{\ j}(\partial_l J^i_{\ k} - \partial_k J^i_{\ l}) - J^l_{\ k}(\partial_l J^i_{\ j} - \partial_j J^i_{\ l})$.

Definition 2.1.7 *An almost complex structure J is a complex structure if its associated Niejenhuis tensor N_J vanishes. Then there exists a holomorphic atlas such that $J_\mu^{\ \nu} = i\delta_\mu^{\ \nu}$, $J_{\bar\mu}^{\ \bar\nu} = -i\delta_{\bar\mu}^{\ \bar\nu}$, $J_{\bar\mu}^{\ \nu} = J_\mu^{\ \bar\nu} = 0$.*

This is a result of the theorem of Newlander and Nirenberg, which states that an almost complex structure J is integrable if and only if its associated Niejenhuis tensor N_J vanishes. They proved that if J is integrable, then there exist local complex coordinates with holomorphic transition functions. We direct the readers to consult [21] for proof. Notice that one fixes the complex structure by specifying the choice of the local coordinates. Often in practice, one can obtain the same topological space or manifolds with different choices of complex coordinates and thus different complex structures (i.e. the torus but with different radii). This leads to the notion of moduli space, which will be discussed briefly in later chapters.

2.1.2 Holomorphic and Anti-Holomorphic vectors

Consider a m-dimensional complex manifold $\mathcal{M}$ with the complex structure J. Equation (2.14) hints that the tangent space at point p, $T_p\mathcal{M}^{\mathbb{C}}$, can be decomposed into the tangent space of holomorphic and anti-holomorphic vectors. Let us define a vector $V \in T_p\mathcal{M}^{\mathbb{C}}$, $V = V^\mu \frac{\partial}{\partial z^\mu}$. Similarly, we define another vector $\bar V \in T_p\mathcal{M}^{\mathbb{C}}$, $\bar V = \bar V^{\bar\mu}\frac{\partial}{\partial z^{\bar\mu}}$. From (2.14), we get $JV = iV$ and $J\bar V = -i\bar V$. Thus, we can decom-

pose the $T_p\mathcal{M}^{\mathbb{C}}$ into two disjoint vector spaces,

$$T_p\mathcal{M}^{\mathbb{C}} = T_p\mathcal{M}^{+} \oplus T_p\mathcal{M}^{-}, \tag{2.20}$$

where

$$T_p\mathcal{M}^{\pm} = \{V \in T_p\mathcal{M}^{\mathbb{C}} : JV = \pm iV\}. \tag{2.21}$$

The space $T_p\mathcal{M}^{+}$ and $T_p\mathcal{M}^{-}$ are spanned by the basis vectors $\{\partial/\partial z^{\mu}\}$ and $\{\partial/\partial z^{\bar{\mu}}\}$ respectively. We call the vectors on $T_p\mathcal{M}^{+}$ holomorphic vectors, and the vectors on $T_p\mathcal{M}^{-}$ anti-holomorphic vectors. We see that any vectors on $T_p\mathcal{M}^{\mathbb{C}}$ can be uniquely decomposed into a sum of holomorphic and anti-holomorphic vectors. Consider the vector $Z = V + \bar{V}$. We act the projection operators from equation (2.15) on Z,

$$PZ = \frac{1}{2}(\mathbb{I}_{2m} - iJ)(V^{\mu}\frac{\partial}{\partial z^{\mu}} + \bar{V}^{\bar{\mu}}\frac{\partial}{\partial z^{\bar{\mu}}}) \tag{2.22}$$

$$= \frac{1}{2}[V^{\mu}\frac{\partial}{\partial z^{\mu}} + \bar{V}^{\bar{\mu}}\frac{\partial}{\partial z^{\bar{\mu}}} + V^{\mu}\frac{\partial}{\partial z^{\mu}} - \bar{V}^{\bar{\mu}}\frac{\partial}{\partial z^{\bar{\mu}}}] \tag{2.23}$$

$$= V \in T_p\mathcal{M}^{+}. \tag{2.24}$$

Similarly $QZ = \bar{V} \in T_p\mathcal{M}^{-}$. Indeed, we see that P and Q projects out the holomorphic and anti-holomorphic vector respectively.

2.1.3 Complex Differential Forms

We can naturally split a one-form into two components with the projection operators. Consider a one-form $w = w_a dx^a$,

$$w = w_a dx^a = (P + Q)w_a dx^a = w^{(1,0)} + w^{(0,1)} \tag{2.25}$$

Here $w^{(1,0)} = Pw$ is called a (1,0)-form, while $w^{(0,1)} = Qw$ is called a (0,1)-form. Similarly, we can split a two-form v into a (2,0), (1,1) and (0,2)-form.

$$v = (P + Q)(P + Q)v = PPv + PQv + QPv + QQv = v^{(2,0)} + v^{(1,1)} + v^{(0,2)} \tag{2.26}$$

where

$$v^{(2,0)}_{mn} = P_m{}^i P_n{}^j v_{ij} \tag{2.27}$$

$$v_{mn}^{(1,1)} = 2P_m{}^i Q_m{}^i v_{ij} \tag{2.28}$$

$$v_{mn}^{(0,2)} = Q_m{}^i Q_n{}^j v_{ij}. \tag{2.29}$$

We can think of a (p,q)-form being a differential form with p holomorphic components and q anti-holomorphic components. Generalising this to a k-form w,

$$w = \sum_{p+q=k} w^{(p,q)}. \tag{2.30}$$

We would like to find a set of basis that can represent a (p,q)-form. Consider a complex one-form $w = w_\mu dz^\mu$, one finds $w = (P+Q)w = Pw$ as $< dz^\mu, \frac{\partial}{\partial z^{\bar{\mu}}} >= 0$. Thus the complex dual basis dz^μ is a (1,0)-form. Going through the same procedure, one finds $dz^{\bar{\mu}}$ being a (0,1)-form. With the dual basis, one can write a (p,q)-form,

$$w = \frac{1}{p!q!} w_{\mu_1 \ldots \mu_p \bar{\nu}_1 \ldots \bar{\nu}_q} dz^{\mu_1} \wedge \ldots \wedge dz^{\mu_p} \wedge dz^{\bar{\nu}_1} \wedge \ldots \wedge dz^{\bar{\nu}_q}. \tag{2.31}$$

The set $\{dz^{\mu_1} \wedge \ldots \wedge dz^{\mu_p} \wedge dz^{\bar{\nu}_1} \wedge \ldots \wedge dz^{\bar{\nu}_q}\}$ forms the basis of the (p,q)-forms. We denote the space of (p,q)-forms on manifold $\mathcal{M}$ as $\Omega^{(p,q)}(\mathcal{M})$.

Restricting ourselves to complex manifolds $\mathcal{M}$[2] and taking the exterior derivative on a (p,q)-form, we get $dw^{(p,q)} = (dw)^{(p,q+1)} + (dw)^{(p+1,q)}$. It implies that the exterior derivative can be decomposed into $d = \partial + \bar{\partial}$, where

$$\partial : \Omega^{(p,q)}(\mathcal{M}) \to \Omega^{(p+1,q)}(\mathcal{M}), \quad \bar{\partial} : \Omega^{(p,q)}(\mathcal{M}) \to \Omega^{(p,q+1)}(\mathcal{M}). \tag{2.32}$$

These operators are called Dolbeault operators. With identity $d^2 = 0$, one finds

$$d^2 w^{(p,q)} = (\partial + \bar{\partial})(\partial + \bar{\partial}) w^{(p,q)} = (\partial^2 + \partial\bar{\partial} + \bar{\partial}\partial + \bar{\partial}^2) w^{(p,q)} = 0 \tag{2.33}$$

$$\partial^2 = \bar{\partial}^2 = (\partial\bar{\partial} + \bar{\partial}\partial) = 0. \tag{2.34}$$

One can show $\partial^2 = 0$ implies that the Niejenhuis tensor vanishes.

[2]On an almost complex manifold, we can decompose the exterior derivative into four components. Taking the exterior derivative on a (p,q)-form, we have a $(p-1, q+2)$-form and a $(p+2, q-1)$-form in addition to the $(p+1, q)$ and $(p, q+1)$-form. We refer the readers to *Complex Manifolds without Potential Theory* by Chern for a detailed discussion.

We can build a real operator d^c, which sends a k-form to a $(k+1)$-form with the Dolbeault operators. We define $d^c = i(\bar{\partial} - \partial)$, which has properties,

$$dd^c + d^c d = 0, \quad (d^c)^2 = 0, \quad \partial = \frac{1}{2}(d + id^c), \quad \bar{\partial} = \frac{1}{2}(d - id^c), \quad dd^c = 2i\partial\bar{\partial}. \tag{2.35}$$

One can then show

$$\partial\bar{\partial} = \frac{1}{4}(d + id^c)(d - id^c) \tag{2.36}$$

$$= \frac{i}{4}(d^c d - dd^c) = -\frac{i}{2}(dd^c) \tag{2.37}$$

$$= -\frac{1}{2}d(\partial - \bar{\partial}) \tag{2.38}$$

which will be useful in showing Ricci-form being closed later.

Definition 2.1.8 *On complex manifold $\mathcal{M}$, a $(p,0)$-form $w \in \Omega^{(p,0)}(\mathcal{M})$ satisfying $\bar{\partial}w = 0$ is called a holomorphic p-form. Likewise, a $(0,q)$-form $v \in \Omega^{(0,q)}(\mathcal{M})$ satisfying $\partial v = 0$ is called an anti-holomorphic q-form.*

The components of the holomorphic and anti-holomorphic forms are holomorphic and anti-holomorphic functions on a local coordinate patch, respectively.

Definition 2.1.9 *A (p,q)-form $w \in \Omega^{(p,q)}(\mathcal{M})$ is called a $\bar{\partial}$-closed (p,q) form if it satisfies $\bar{\partial}w = 0$. It is called a ∂-closed (p,q) form if it satisfies $\partial w = 0$. It is called a $\bar{\partial}$-exact (p,q) form if it satisfies $w = \bar{\partial}\eta$ for some $\eta \in \Omega^{(p,q-1)}(\mathcal{M})$. It is called a ∂-exact (p,q) form if it satisfies $w = \partial\eta$ for some $\eta \in \Omega^{(p-1,q)}(\mathcal{M})$.*

2.1.4 Cohomology Groups

It is crucial to study the cohomology of a manifold in order to understand its topological properties. On a real manifold, one has the de Rham cohomology which concerns differential forms that are closed but not exact. Knowing the cohomology group of a manifold then allows us to define topological invariants like the Betti numbers and Euler characteristic. On a complex manifold, one can define the analogue of de Rham cohomology, namely the Dolbeault cohomology.

Let us consider a complex manifold $\mathcal{M}$.

Definition 2.1.10 *The (p,q)-cocycle of $\mathcal{M}$ is the set of $\bar{\partial}$-closed (p,q)-forms, denoted by $Z_{\bar{\partial}}^{(p,q)}(\mathcal{M})$. The (p,q)-coboundary of $\mathcal{M}$ is the set of $\bar{\partial}$-exact (p,q)-forms, denoted by $B_{\bar{\partial}}^{(p,q)}(\mathcal{M})$. We define a complex vector space*

$$H_{\bar{\partial}}^{(p,q)}(\mathcal{M}) \equiv Z_{\bar{\partial}}^{(p,q)}(\mathcal{M})/B_{\bar{\partial}}^{(p,q)}(\mathcal{M}) \tag{2.39}$$

called the (p,q)-th $\bar{\partial}$-cohomology group.

An element $[w] \in H_{\bar{\partial}}^{(p,q)}(\mathcal{M})$ is an equivalence class of $\bar{\partial}$-closed (p,q)-forms which differ from w by a $\bar{\partial}$-exact form. One can show the $\bar{\partial}$-cohomology groups of $\mathbb{C}^m$ are trivial with Poincaré lemma, that is, all closed (p,q)-forms are exact. These properties are reminiscent of de Rham cohomology groups, however, one should notice that the Dolbeault cohomology also depends on the complex structure of the manifold, not only on the topological data.

We now define the analogue of Betti numbers on a complex manifold, that is the Hodge numbers. Consider a m-dimensional complex manifold $\mathcal{M}$.

Definition 2.1.11 *The Hodge numbers are defined to be $h^{(p,q)}$=dim $H_{\bar{\partial}}^{(p,q)}(\mathcal{M})$.*

We can summarise the Hodge numbers by defining the Hodge diamond,

$$\begin{pmatrix} & & & h^{(m,m)} & & & \\ & & h^{(m,m-1)} & \vdots & h^{(m-1,m)} & & \\ h^{(m,0)} & h^{(m-1,1)} & & \cdots & & h^{(1,m-1)} & h^{(0,m)} \\ & & h^{(1,0)} & \vdots & h^{(0,1)} & & \\ & & & h^{(0,0)} & & & \end{pmatrix} \tag{2.40}$$

We have $(m+1)^2$ Hodge numbers in the diamond, and most of them are not independent. The Hodge numbers share different kinds of relations among themselves, depending on the type of manifold they are on. For instance on a Kähler manifold, (see [18] for proof) the Hodge numbers satisfy $h^{(p,q)} = h^{(q,p)}$ and $h^{(p,q)} = h^{(m-p,m-q)}$.

Recall the Betti numbers on real manifolds are defined as $b^k = \dim_{\mathbb{R}} H^k_{dR}(M, \mathbb{R})$, where we denote de Rham cohomology group of k-forms on real manifold M as $H^k_{dR}(M)$. There is a useful relation between Betti numbers and Hodge numbers,

$$b^k = \sum_{p+q=k} h^{(p,q)}, \tag{2.41}$$

which allows us to rewrite the Euler characteristic,

$$\chi = \sum_{p,q} (-1)^{p+q} h^{p,q}. \tag{2.42}$$

2.1.5 Hermitian and Kähler Manifolds

We start by defining a Hermitian manifold on a complex manifold $\mathcal{M}$ with a complex structure J and a Riemannian metric g. Cohomology classes defined in this chapter are Dolbeault cohomology classes unless otherwise specified.

Definition 2.1.12 *A complex manifold is Hermitian if it is endowed with a metric of the form $ds^2 = g_{\mu\bar{\nu}} dz^\mu dz^{\bar{\nu}}$. We call this metric a hermitian metric, which obeys $g_{mn} = J_m{}^k J_n{}^l g_{kl}$.*

We can write the most general form of the metric as $ds^2 = g_{\mu\bar{\nu}} dz^\mu dz^{\bar{\nu}} + g_{\mu\nu} dz^\mu dz^\nu + g_{\bar{\mu}\bar{\nu}} dz^{\bar{\mu}} dz^{\bar{\nu}}$. This leads to an alternative definition of a Hermitian metric, that is Hermitian metric has vanishing pure holomorphic and pure anti-holomorphic components, i.e. $g_{\mu\nu} = g_{\bar{\mu}\bar{\nu}} = 0$. Notice that hermiticity restricts only the metric of the manifold, not the manifold itself. One can show the complex structure is anti-symmetric on a Hermitian manifold,

$$g_{mn} = J_m{}^k J_n{}^l g_{kl} \tag{2.43}$$

$$J_k{}^m g_{mn} = J_k{}^m J_m{}^k J_n{}^l g_{kl} \tag{2.44}$$

$$J_{kn} = -J_n{}^l g_{kl} = -J_{nk} \tag{2.45}$$

where we have used the identity (2.9) on equation (2.44). Thus, the complex structure defines a natural two-form on a Hermitian manifold, called the Kähler form, or

sometimes called the Hermitian two-form.

Definition 2.1.13 *On a Hermitian manifold $\mathcal{M}$ with a complex structure J and hermitian metric g, we define the Kähler form as*

$$w(X,Y) = g(JX,Y) \qquad X,Y \in T_p\mathcal{M} \tag{2.46}$$

In local coordinates, the Kähler form is written as $w_{ab} = J_a{}^c g_{cb}$. In a complex basis, one can write the Kähler form $w = ig_{\mu\bar{\nu}} dz^\mu \wedge dz^{\bar{\nu}}$, which is a (1,1)-form.

On a complex manifold with Riemannian metric h, we can define an object

$$g_{mn} = \frac{1}{2}(h_{mn} + J_m{}^k J_n{}^l h_{kl}). \tag{2.47}$$

g is by construction positive definite as h is a Riemannian metric. Then,

$$J_m{}^k J_n{}^l g_{kl} = \frac{1}{2}(h_{kl} + J_k{}^a J_l{}^b h_{ab}) J_m{}^k J_n{}^l \tag{2.48}$$

$$= \frac{1}{2}(J_m{}^k J_n{}^l h_{kl} + \delta^a_m \delta^b_n h_{ab}) = g_{mn} \tag{2.49}$$

concludes that g_{mn} is a Hermitian metric. This proves that it is always possible to find a Hermitian metric on a complex manifold.

To study the geometry of Hermitian manifolds, one needs to know its connections. Recall that on a real manifold, one determines the Christoffel connection by requiring the metric to be covariantly constant and symmetric. However to specify a connection on Hermitian manifolds, one needs to require both the complex structure and the metric to be covariantly constant.

Definition 2.1.14 *Let ($\mathcal{M}$,J,g) be a Hermitian manifold. The hermitian connection is a metric connection such that $\nabla g = \nabla J = 0$.*

In local coordinates, one finds

$$\partial_a g_{bc} - \Gamma_{ab}{}^d g_{dc} - \Gamma_{ac}{}^d g_{bd} = 0 \tag{2.50}$$

$$\partial_a J_b{}^c + \Gamma_{ad}{}^c J_b{}^d - \Gamma_{ab}{}^d J_d{}^c = 0. \tag{2.51}$$

We take $(b,c) = (\mu, \bar{\nu})$ on equation (2.51),

$$\Gamma_{ad}{}^{\bar{\nu}} J_{\mu}{}^{d} - \Gamma_{a\mu}{}^{d} J_{d}{}^{\bar{\nu}} = \Gamma_{a\rho}{}^{\bar{\nu}} J_{\mu}{}^{\rho} - \Gamma_{a\mu}{}^{\bar{\rho}} J_{\bar{\rho}}{}^{\bar{\nu}} = 2i\Gamma_{a\mu}{}^{\bar{\nu}} = 0 \tag{2.52}$$

and yields $\Gamma_{\kappa\mu}{}^{\bar{\nu}} = \Gamma_{\bar{\kappa}\mu}{}^{\bar{\nu}} = 0$. Taking the complex conjugates (i.e. $(b,c) = (\bar{\mu}, \nu)$), one also gets $\Gamma_{\bar{\kappa}\bar{\mu}}{}^{\nu} = \Gamma_{\kappa\bar{\mu}}{}^{\nu} = 0$.

Recall that the components of the torsion are given by $\Gamma_{[ab]}{}^{c} \equiv \Gamma_{ab}{}^{c} - \Gamma_{ba}{}^{c}$. To define a unique hermitian connection, one needs to further impose that the torsion is pure in its lower indices (i.e. $\Gamma_{[\kappa\bar{\mu}]}{}^{\nu} = 0$). This implies the connection is symmetric if its lower indices are mixed. With the previously obtained vanishing components, we get $\Gamma_{\bar{\kappa}\mu}{}^{\bar{\nu}} = \Gamma_{\mu\bar{\kappa}}{}^{\bar{\nu}} = 0$ and $\Gamma_{\kappa\bar{\mu}}{}^{\nu} = \Gamma_{\bar{\mu}\kappa}{}^{\nu} = 0$. Thus, all mixed components of the connection vanish and we are left with $\Gamma_{\kappa\mu}{}^{\nu}$ and $\Gamma_{\bar{\kappa}\bar{\mu}}{}^{\bar{\nu}}$. The connection being pure in its indices implies that a holomorphic/anti-holomorphic vector remains holomorphic/anti-holomorphic after parallel transport, and thus preserves holomorphicity and imposes a restriction on its holonomy.

One can check that imposing the conditions $\nabla_{\bar{\mu}} w^{\nu} = \partial_{\bar{\mu}} w^{\nu}$ and $\nabla_{\mu} w^{\bar{\nu}} = \partial_{\mu} w^{\bar{\nu}}$ also yields the results above ($\Gamma_{\bar{\mu}\kappa}{}^{\nu} = 0$ and $\Gamma_{\mu\bar{\kappa}}{}^{\bar{\nu}} = 0$). The connection that satisfies these two relations is called a Chern connection.

We now turn our focus to equation (2.50). Taking $(a,b,c) = (\mu, \nu, \bar{\rho})$, we have

$$\partial_{\mu} g_{\nu\bar{\rho}} - \Gamma_{\mu\nu}{}^{\kappa} g_{\kappa\bar{\rho}} = 0 \tag{2.53}$$

$$\Gamma_{\mu\nu}{}^{\kappa} = g^{\kappa\bar{\rho}} \partial_{\mu} g_{\nu\bar{\rho}}. \tag{2.54}$$

Similarly with $(a,b,c) = (\bar{\mu}, \bar{\nu}, \rho)$, one finds

$$\Gamma_{\bar{\mu}\bar{\nu}}{}^{\bar{\kappa}} = g^{\bar{\kappa}\rho} \partial_{\bar{\mu}} g_{\bar{\nu}\rho}. \tag{2.55}$$

In contrast to the Christoffel connection, the Hermitian connection is not symmetric. However, the Hermitian connection gives us a simple Riemman tensor structure. Recall the expression for the Riemann tensor,

$$R_{mn}{}^{k}{}_{l} = \partial_{m} \Gamma_{nl}{}^{k} - \partial_{n} \Gamma_{ml}{}^{k} + \Gamma_{mr}{}^{k} \Gamma_{nl}{}^{r} - \Gamma_{nr}{}^{k} \Gamma_{ml}{}^{r}. \tag{2.56}$$

The Riemann tensor vanishes for $(k,l) = (\bar{\kappa}, \lambda)$ since the connection with mixed indices is trivial. Thus, $R_{mn\kappa\lambda} = g_{\kappa\bar{\rho}} R_{mn}{}^{\bar{\rho}}{}_{\lambda} = 0$. This also holds for its complex conjugate. Similarly, the Riemann tensor vanishes for $(m,n,k,l) = (\mu, \nu, \bar{\kappa}, \bar{\lambda})$. Finally, consider $(m,n,k,l) = (\mu, \nu, \kappa, \lambda)$,

$$R_{\mu\nu}{}^{\kappa}{}_{\lambda} = \partial_{\mu}\Gamma_{\nu\lambda}{}^{\kappa} + \Gamma_{\mu\rho}{}^{\kappa}\Gamma_{\nu\lambda}{}^{\rho} - (\mu \leftrightarrow \nu) \tag{2.57}$$

$$= \partial_{\mu}(g^{\kappa\bar{\rho}}\partial_{\nu}g_{\lambda\bar{\rho}}) + (g^{\kappa\bar{\alpha}}\partial_{\mu}g_{\rho\bar{\alpha}})(g^{\rho\bar{\sigma}}\partial_{\nu}g_{\lambda\bar{\sigma}}) - (\mu \leftrightarrow \nu) \tag{2.58}$$

$$= \partial_{\mu}g^{\kappa\bar{\rho}}\partial_{\nu}g_{\lambda\bar{\rho}} + (-g_{\rho\bar{\alpha}}\partial_{\mu}g^{\kappa\bar{\alpha}})(g^{\rho\bar{\sigma}}\partial_{\nu}g_{\lambda\bar{\sigma}}) + g^{\kappa\bar{\rho}}\partial_{\mu}\partial_{\nu}g_{\lambda\bar{\rho}} - (\mu \leftrightarrow \nu) \tag{2.59}$$

$$= g^{\kappa\bar{\rho}}\partial_{\mu}\partial_{\nu}g_{\lambda\bar{\rho}} - g^{\kappa\bar{\rho}}\partial_{\nu}\partial_{\mu}g_{\lambda\bar{\rho}} = 0 \tag{2.60}$$

where we have used the identity $g^{\kappa\bar{\alpha}}\partial_{\mu}g_{\rho\bar{\alpha}} = -g_{\rho\bar{\alpha}}\partial_{\mu}g^{\kappa\bar{\alpha}}$ on equation (2.58), derived from $\partial_{\mu}(\delta^{\kappa}_{\rho}) = \partial_{\mu}(g_{\rho\bar{\alpha}}g^{\bar{\alpha}\kappa}) = 0$.

We are left with the Riemann tensor of form $R_{\bar{\mu}\nu}{}^{\kappa}{}_{\lambda}$ and $R_{\mu\bar{\nu}}{}^{\bar{\kappa}}{}_{\bar{\lambda}}$. Thus, the independent non-zero components of the Riemann tensor are

$$R_{\bar{\mu}\nu}{}^{\kappa}{}_{\lambda} = \partial_{\bar{\mu}}\Gamma_{\nu\lambda}{}^{\kappa} = \partial_{\bar{\mu}}(g^{\kappa\bar{\rho}}\partial_{\nu}g_{\lambda\bar{\rho}}) \tag{2.61}$$

$$R_{\mu\bar{\nu}}{}^{\bar{\kappa}}{}_{\bar{\lambda}} = \partial_{\mu}\Gamma_{\bar{\nu}\bar{\lambda}}{}^{\bar{\kappa}} = \partial_{\mu}(g^{\bar{\kappa}\rho}\partial_{\bar{\nu}}g_{\bar{\lambda}\rho}) \tag{2.62}$$

One can verify the symmetries $R_{\bar{\mu}\nu\bar{\kappa}\lambda} = g_{\bar{\kappa}\sigma}R_{\bar{\mu}\nu}{}^{\sigma}{}_{\lambda} = -R_{\nu\bar{\mu}\bar{\kappa}\lambda}$ and $R_{\bar{\mu}\nu\bar{\kappa}\lambda} = -R_{\bar{\mu}\nu\lambda\bar{\kappa}}$.

Contracting the Riemann tensor gives us the Ricci tensor. Differs from real geometry, one can use the complex structure to contract the Riemann tensor and yield the Ricci-form $\mathcal{R}$, defined by

$$\mathcal{R} \equiv \frac{1}{4}R_{mnkl}J^{kl}dx^{m} \wedge dx^{n} \equiv i\mathcal{R}_{\mu\bar{\nu}}dz^{\mu} \wedge dz^{\bar{\nu}} \tag{2.63}$$

$$= \frac{1}{4}(R_{\mu\bar{\nu}kl}J^{kl}dz^{\mu} \wedge dz^{\bar{\nu}} + R_{\bar{\nu}\mu kl}J^{kl}dz^{\bar{\nu}} \wedge dz^{\mu}) = \frac{1}{2}R_{\mu\bar{\nu}kl}J^{kl}dz^{\mu} \wedge dz^{\bar{\nu}} \tag{2.64}$$

$$= \frac{1}{2}(R_{\mu\bar{\nu}\kappa\bar{\lambda}}g^{\kappa\bar{\alpha}}J_{\bar{\alpha}}{}^{\bar{\lambda}} + R_{\mu\bar{\nu}\bar{\kappa}\lambda}g^{\bar{\kappa}\alpha}J_{\alpha}{}^{\lambda})dz^{\mu} \wedge dz^{\bar{\nu}} \tag{2.65}$$

$$= \frac{i}{2}(R_{\mu\bar{\nu}}{}^{\rho}{}_{\rho} - R_{\mu\bar{\nu}}{}^{\bar{\rho}}{}_{\bar{\rho}})dz^{\mu} \wedge dz^{\bar{\nu}}. \tag{2.66}$$

The Ricci-form is a (1,1)-form. Now the metric is of form $g_{mn} = \left(\begin{smallmatrix} 0 & g_{\mu\bar{\nu}} \\ g_{\rho\bar{\sigma}} & 0 \end{smallmatrix}\right)$, we define

$G \equiv \det(g_{\mu\bar{\nu}}) = \sqrt{g}$, and use the identity $\delta G = G g^{\mu\bar{\nu}} \delta g_{\mu\bar{\nu}}$ to obtain,

$$R_{\mu\bar{\nu}}{}^{\rho}{}_{\rho} = -\partial_{\bar{\nu}} \Gamma_{\mu\rho}{}^{\rho} = -\partial_{\bar{\nu}} (g^{\rho\bar{\sigma}} \partial_{\mu} g_{\rho\bar{\sigma}}) = -\partial_{\bar{\nu}} \partial_{\mu} \log G \tag{2.67}$$

$$R_{\mu\bar{\nu}}{}^{\bar{\rho}}{}_{\bar{\rho}} = \partial_{\bar{\nu}} \partial_{\mu} \log G. \tag{2.68}$$

Thus, we can write the Ricci-form

$$\mathcal{R} = -i\partial\bar{\partial} \log G, \quad \mathcal{R}_{\mu\bar{\nu}} \equiv R_{\mu\bar{\nu}}{}^{\rho}{}_{\rho} = -\partial_{\mu}\partial_{\bar{\nu}} \log G. \tag{2.69}$$

Recall from equation (2.38), $\partial\bar{\partial} = -\frac{1}{2} d(\partial - \bar{\partial})$. We immediately see that the Ricci-form is closed $d\mathcal{R} = 0$. One might naively think that the Ricci-form is also exact. However, in general, G and thus $(\partial - \bar{\partial}) \log G$ is not a coordinate scalar. Therefore, $\mathcal{R}_{\mu\bar{\nu}}$ of (2.69) only holds locally on a coordinate patch. Despite $\log G$ not being defined globally, one can still show $\mathcal{R}$ is. Consider the variation of the Ricci-form,

$$\delta\mathcal{R} = \delta(i\partial\bar{\partial} \log G) = i\partial\bar{\partial}(g^{\mu\bar{\nu}} \delta g_{\mu\bar{\nu}}) = -\frac{i}{2} d[(\partial - \bar{\partial}) g^{\mu\bar{\nu}} \delta g_{\mu\bar{\nu}}]. \tag{2.70}$$

This shows that $\delta\mathcal{R}$ is exact as $g^{\mu\bar{\nu}} \delta g_{\mu\bar{\nu}}$ is a coordinate scalar. It implies that $\mathcal{R}$ defines a cohomology class,

$$c_1 = \left[\frac{1}{2\pi}\mathcal{R}\right] \tag{2.71}$$

called the first Chern class. In addition, the variation is an exact form implies that c_1 is an analytic invariant (i.e. $[\mathcal{R}] = [\mathcal{R} + \delta\mathcal{R}]$). Thus, the first Chern class is invariant under smooth variation of the complex structure of the manifold.

The above concludes the geometry of Hermitian manifolds. Let us now turn to Kähler manifolds.

Definition 2.1.15 *A Hermitian manifold (M,J,g) is a Kähler manifold if its Kähler form w is closed, $dw = 0$. Then the metric on the manifold is called Kähler.*

Recall the Kähler form can be written as $w = i g_{\mu\bar{\nu}} dz^{\mu} \wedge dz^{\bar{\nu}}$, then

$$dw = (\partial + \bar{\partial}) w = i\partial_{\kappa} g_{\mu\bar{\nu}} dz^{\kappa} \wedge dz^{\mu} \wedge dz^{\bar{\nu}} - i\partial_{\bar{\rho}} g_{\mu\bar{\nu}} dz^{\mu} \wedge dz^{\bar{\rho}} \wedge dz^{\bar{\nu}} \tag{2.72}$$

$$0 = \frac{i}{2}(\partial_\kappa g_{\mu\bar{\nu}} - \partial_\mu g_{\kappa\bar{\nu}})dz^\kappa \wedge dz^\mu \wedge dz^{\bar{\nu}} - \frac{i}{2}(\partial_{\bar{\rho}} g_{\mu\bar{\nu}} - \partial_{\bar{\nu}} g_{\mu\bar{\rho}})dz^\mu \wedge dz^{\bar{\rho}} \wedge dz^{\bar{\nu}}. \quad (2.73)$$

Thus on a Kähler manifold, one finds the useful identity

$$\partial_\kappa g_{\mu\bar{\nu}} = \partial_\mu g_{\kappa\bar{\nu}} \quad \text{and} \quad \partial_{\bar{\rho}} g_{\mu\bar{\nu}} = \partial_{\bar{\nu}} g_{\mu\bar{\rho}}. \quad (2.74)$$

called the Kähler condition. Together with equations (2.54) and (2.55), one finds that the Hermitian connection is symmetric on its bottom two indices, and thus the torsion completely vanishes. It also implies $\nabla w = dw$ for any p-forms w. Furthermore, the Riemann tensor has an additional symmetry, $R_{\bar{\mu}\nu}{}^{\kappa}{}_{\lambda} = R_{\bar{\mu}\lambda}{}^{\kappa}{}_{\nu}$ and $R_{\mu\bar{\nu}}{}^{\bar{\kappa}}{}_{\bar{\lambda}} = R_{\mu\bar{\lambda}}{}^{\bar{\kappa}}{}_{\bar{\nu}}$.

With the new symmetry on the Riemann tensor, one finds the Ricci tensor coincides with the components of the Ricci-form (2.69), i.e. $\mathcal{R}_{\mu\bar{\nu}} = R_{\mu\bar{\nu}}{}^{\rho}{}_{\rho} = R_{\rho\bar{\nu}}{}^{\rho}{}_{\mu} = R_{\mu\bar{\nu}}$. Therefore, a Kähler manifold is Ricci-flat if it has a vanishing Ricci-form, which further implies a vanishing first Chern-class.

One important consequence of Kählerity is that it allows us to define the metric in terms of Kähler potentials. Recall the Poincaŕe's lemma, which states that on a contractible coordinate patch, any closed r-form is also exact. Extending to complex manifolds on contractible coordinate patches, any closed (p, q)-form can be written as $\alpha = \partial\bar{\partial}\eta$ where η is some $(p-1, q-1)$-form. This implies that our Kähler (1,1)-form w can be locally expressed as $w_{\mu\bar{\nu}} = \partial_\mu \bar{\partial}_\nu \mathcal{K}$, $w = i\partial\bar{\partial}\mathcal{K}$, where $\mathcal{K}$ is a scalar function of $(z, \bar{z})$ called the Kähler potential. We now have two expressions for the Kähler form in local coordinates. By comparing the two,

$$w_{\mu\bar{\nu}} = g_{\mu\bar{\nu}} = \partial_\mu \partial_{\bar{\nu}} \mathcal{K}. \quad (2.75)$$

Clearly, the Kähler potential is not uniquely determined. One can obtain the same metric with two different Kähler potentials, $\mathcal{K}$ and $\mathcal{K} + f + \bar{f}$ on the same coordinate patch, where f and $\bar{f}$ is any holomorphic and anti-holomorphic function respectively. It follows from the fact that $\partial\bar{\partial}(f + \bar{f}) = 0$.

Consider a non-trivial overlapping coordinate chart region $U \cap U^{'}$ on a Kähler manifold. The Kähler metric, defined via $\partial_\mu \partial_{\bar{\nu}} \mathcal{K}$ and $\partial_\mu \partial_{\bar{\nu}} \mathcal{K}^{'}$ on the chart U and $U^{'}$ respectively, should agree with each other. This implies that on Kähler manifolds, the Kähler potentials on different coordinate patches satisfy the relation, $\mathcal{K}^{'} = \mathcal{K} + f + \bar{f}$, called the Kähler transformation. Manifold is not Kähler if we cannot find a globally defined Kähler potential up to a Kähler transformation.

Similar to the Ricci-form, one might naively think that the Kähler form $w = i\partial\bar{\partial}\mathcal{K}_j = -\frac{i}{2} d[(\partial - \bar{\partial})\mathcal{K}_j]$ is both closed and exact. However, we will show that this is not the case, and thus it defines a cohomology class. Consider taking the wedge product[3] of $w = i g_{\mu\bar{\nu}} dz^\mu \wedge dz^{\bar{\nu}}$ m-times on a $m-$dimensional Kähler manifold,

$$w \wedge \cdots \wedge w = i^m g_{\mu_1 \bar{\nu}_1} \ldots g_{\mu_m \bar{\nu}_m} dz^{\mu_1} dz^{\bar{\nu}_1} \ldots dz^{\mu_m} dz^{\bar{\nu}_m} \tag{2.76}$$

$$= i^m \epsilon^{\mu_1 \ldots \mu_m} \epsilon^{\bar{\nu}_1 \ldots \bar{\nu}_m} g_{\mu_1 \bar{\nu}_1} \ldots g_{\mu_m \bar{\nu}_m} dz^1 dz^{\bar{1}} \ldots dz^m dz^{\bar{m}} \tag{2.77}$$

$$= i^m m! \det(g_{\mu\bar{\nu}}) dz^1 dz^{\bar{1}} \ldots dz^m dz^{\bar{m}}. \tag{2.78}$$

We see that the m-fold product of the Kähler form, which is a top-form of the manifold, is nowhere vanishing. Therefore, it defines a volume element and thus proves that complex manifolds are orientable.

Since $w \wedge \cdots \wedge w$ is proportional to the volume form, the volume of the manifold, up to a proportionality constant, can be found by evaluating the integral $\int w \wedge \cdots \wedge w$. However, if the Kähler form is exact, that is $w = dA$, the integral vanishes by substituting one of the w to be dA and invoking Stoke's theorem. Hence, the Kähler form cannot be exact, and the set of Kähler forms w defines a cohomology class $[w]$, called the Kähler class. Similar to the complex structure moduli mentioned earlier, the Kähler class and Kähler potentials define a Kähler moduli space (or called the Kähler cone) which will be discussed briefly in later chapters.

[3]Here we adopt the shorthand notation i.e. $dz^1 \wedge dz^2 \wedge dz^3 = dz^1 dz^2 dz^3$.

2.1.6 Holonomy on Kähler Manifolds

As mentioned earlier, the connection on a Kähler manifold has no components with mixed indices. Therefore, parallel transport on Kähler manifolds preserves the holomorphicity and length of a vector. This tells us that the holonomy groups on m-dimensional Kähler manifolds are subgroups of $U(m) \subset SO(2m)$.

If the Kähler manifold admits a Ricci-flat metric, then its holonomy group is contained in $SU(m)$ instead. Consider a vector V^k parallel transported around an infinitesimal parallelogram of area δa^{mn} with edges parallel to the vectors $\frac{\partial}{\partial x^m}$ and $\frac{\partial}{\partial x^n}$,

$$V'^k = V^k + \delta a^{mn} R_{mn}{}^k{}_l V^l = (\delta^k{}_l + \delta a^{mn} R_{mn}{}^k{}_l) V^l = h^k{}_l V^l. \tag{2.79}$$

In the vicinity of the identity, one can decompose $U(m) = SU(m) \times U(1)$. We know the matrix $h^k{}_l$ is in $U(m)$, and thus the matrix $\delta a^{mn} R_{mn}{}^k{}_l$ is in the Lie algebra of $U(m)$. Consider decomposing the Lie algebra $\mathfrak{u}(m) = \mathfrak{su}(m) \oplus \mathfrak{u}(1)$, where $\mathfrak{su}(m)$ is traceless and $\mathfrak{u}(1)$ is a trace. The $\mathfrak{u}(1)$ element is generated by

$$\delta^k{}_l + \delta a^{mn} R_{mn}{}^k{}_k = -4\delta a^{\mu\bar{\nu}} R_{\mu\bar{\nu}}. \tag{2.80}$$

If the Kähler manifold is Ricci-flat, the Ricci tensor vanishes and $\mathfrak{u}(1)$ is trivial. Thus, the holonomy of a Ricci-flat Kähler manifold is a subgroup of SU(m). Remarkably, SU(m) holonomy implies the existence of covariant constant spinors, which is crucial for superstring compactification.

Example: Kähler Potentials and Revisiting $\mathbb{CP}^N$

Let us try to find the Kähler potentials on $\mathbb{C}^m$ to illustrate the idea of Kähler potentials concretely. The metric components on $\mathbb{C}^m$ are $g_{\mu\nu} = g_{\bar{\mu}\bar{\nu}} = 0$ and $g_{\mu\bar{\nu}} = g_{\bar{\mu}\nu} = \frac{1}{2}\delta_{\mu\bar{\nu}}$. Therefore, the Kähler form is $w = ig_{\mu\bar{\nu}} dz^\mu \wedge dz^{\bar{\nu}} = \frac{i}{2}\sum_{\mu=1}^{m} dz^\mu \wedge dz^{\bar{\mu}}$, which clearly satisfies $dw = 0$. Let $\mathcal{K}$ be the Kähler potential, such that $w = i\partial\bar{\partial}\mathcal{K}$. Thus, we find the Kähler potential, $\mathcal{K} = \frac{1}{2}\sum z^\mu z^{\bar{\mu}}$.

The complex projective space $\mathbb{CP}^N$ defined in ch 2.1 is Kähler. Recall that on coordinate patch $U_{(i)}$, the inhomogeneous coordinates are defined to be

$$\zeta^\mu_{(i)} = \frac{z^\mu}{z^i}. \tag{2.81}$$

To prove $\mathbb{CP}^N$ is Kähler, one has to show that it admits a closed Kähler form and that the Kähler metric is Hermitian and satisfies the Kähler conditions. Let us choose an ansatz for the metric that satisfies the Kähler conditions, $g_{\mu\bar{\nu}} = \partial_\mu \partial_{\bar{\nu}} \mathcal{K}_i$, where $\mathcal{K}$ is some scalar function. Let us also make an ansatz for the scalar function $\mathcal{K}$ on the i-th patch,

$$\mathcal{K}_i = \log\left(\sum_{\mu=1}^{n+1} |\zeta^\mu_i|^2\right). \tag{2.82}$$

We see the scalar function is by construction positive-definite. On $U_{(i)} \cap U_{(j)}$, we have $\zeta^\mu_i = \zeta^\mu_j/\zeta^i_j$, then it follows that

$$\mathcal{K}_i = \log\left(\sum_{\mu=1}^{n+1} |\frac{\zeta^\mu_j}{\zeta^i_j}|^2\right) = \log\left(\sum_{\mu=1}^{n+1} |\zeta^\mu_j|^2\right) - \log\left(|\zeta^i_j|^2\right) \tag{2.83}$$

$$= \mathcal{K}_j - \log\left(\zeta^i_j \bar{\zeta}^i_j\right) \tag{2.84}$$

$$\Rightarrow \mathcal{K}_i = \mathcal{K}_j - \log\left(\zeta^i_j\right) - \log\left(\bar{\zeta}^i_j\right). \tag{2.85}$$

This is a Kähler transformation as $\partial\bar{\partial}\mathcal{K}_i = \partial\bar{\partial}\mathcal{K}_j$, and ensures the metric $g_{\mu\bar{\nu}} = \partial_\mu\partial_{\bar{\nu}}\mathcal{K}_i$ being globally defined. It induces the Kähler form,

$$w = i\partial\bar{\partial}\mathcal{K}_i \tag{2.86}$$

which is clearly a closed (1,1)-form. The final step is to show that g is positive-definite, which implies that $\mathcal{K}$ is the Kähler potential, and g is the Kähler metric. We first substitute (2.83) into the metric ansatz and find,

$$g_{\mu\bar{\nu}} = \frac{1}{\sigma}(\delta_{\mu\bar{\nu}} - \frac{\zeta_\mu \zeta_{\bar{\nu}}}{\sigma}), \quad \sigma = 1 + |\zeta|^2 \tag{2.87}$$

where $|\zeta|^2 = \sum_{\mu=1}^n |\zeta^\mu|^2$ and we have dropped the patch indices on ζ^μ_i. Consider a

real vector $v = v^\mu \frac{\partial}{\partial \zeta^\mu} + v^{\bar{\mu}} \frac{\partial}{\partial \zeta^{\bar{\mu}}}$, the inner product with respect to the metric is

$$g_{\mu\bar{\nu}} v^\mu v^{\bar{\nu}} = 2 \sum_{\mu\bar{\nu}} \frac{\delta_{\mu\bar{\nu}} \sigma - \zeta^\mu \zeta^{\bar{\nu}}}{\sigma^2} v^\mu v^{\bar{\nu}}. \tag{2.88}$$

We can show the metric g is positive-definite by applying the Schwarz inequality (i.e. $\sum_\mu |v^\mu|^2 \cdot |\zeta|^2 \geq \sum_\mu |v^\mu \zeta^\mu|^2$). Hence, the metric and thus $\mathbb{CP}^N$ is Kähler. The metric defined here is called the Fubini-Study metric, which is applied intensively in the study of numerical Calabi-Yau metrics.

2.1.7 Vector Bundles

Let us turn our attention to fibre bundles as they appear to be important for understanding characteristic classes and for our discussion on Calabi-Yau metrics. In this chapter, we will state without proof the necessary definitions that lead to the notion of holomorphic vector bundles. We suggest readers consult [18, 20] for detailed proof and discussions. We first define the tangent bundle.

Definition 2.1.16 *For a m-dimensional real manifold $\mathcal{M}$, we define the tangent bundle over $\mathcal{M}$, denoted as $T\mathcal{M}$, as the union of all the tangent spaces of $\mathcal{M}$,*

$$T\mathcal{M} \equiv \bigcup_{p \in \mathcal{M}} T_p \mathcal{M}. \tag{2.89}$$

We call $\mathcal{M}$, where the tangent bundle $T\mathcal{M}$ is defined over, as the base space.

The cotangent bundle is defined similarly, $T^*\mathcal{M} \equiv \bigcup_{p\in\mathcal{M}} T_p^*\mathcal{M}$. Let us construct charts on $\mathcal{M}$ as $\{U_i, \varphi_i\}$, and pick local coordinates $x^\mu = \varphi_i(p)$ on the coordinate patch U_i. The open set U_i is a manifold, and its tangent bundle is defined as

$$TU_i \equiv \bigcup_{p\in U_i} T_p\mathcal{M} \quad \Rightarrow \quad \text{identified with} \qquad TU_i = U_i \times \mathbb{R}^m. \tag{2.90}$$

An element $V_p \in TU_i$ is specified by a point $p \in \mathcal{M}$ and the tangent vector on the point $V = V^\mu(p) \frac{\partial}{\partial x^\mu}|_p \in T_p\mathcal{M}$. Thus, it is straightforward to show the tangent bundle locally is a product manifold homeomorphic to $\mathbb{R}^m \times \mathbb{R}^m = \mathbb{R}^{2m}$, and hence, TU_i and $T\mathcal{M}$ is a $2m$-dimensional differentiable manifold.

As TU_i is decomposable into a direct product $U_i \times \mathbb{R}^m$, it is natural to define a *projection* map $\pi : TU_i \to U_i$. For point $u \in TU_i$, the action $\pi(u)$ gives us the point $p \in U_i$ at which the tangent vector is defined. Clearly, $\pi(u) = p$ is independent of the local coordinate choice. Therefore, the projection map can be defined globally $\pi : T\mathcal{M} \to \mathcal{M}$. Conversely, $\pi^{-1}(p) = T_p\mathcal{M}$. We call $T_p\mathcal{M}$ the *fibre* at point p.

Consider a non-trivial overlapping chart region $U_i \cap U_j$. Let us pick x^μ and y^μ as the local coordinates on patch U_i and U_j respectively. For a vector $V \in T_p\mathcal{M}$,

$$V = V^\mu \frac{\partial}{\partial x^\mu}\Big|_p = \tilde{V}^\nu \frac{\partial}{\partial y^\nu}\Big|_p \quad \Rightarrow \quad \tilde{V}^\nu = \frac{\partial y^\nu}{\partial x^\mu}\Big|_p V^\mu. \tag{2.91}$$

Assuming the choice of coordinates on the two patches is compatible with each other, the matrix $M^\nu_\mu \equiv (\partial y^\nu / \partial x^\mu)$ must be invertible, that is, $M^\nu_\mu \in GL(m, \mathbb{R})$. We call this group the *structure group* of $T\mathcal{M}$. This implies that transition functions on $U_i \cap U_j$ take values in the structure group.

We now relate the notion of *sections* with vector fields.

Definition 2.1.17 *A section (or a cross-section) of a tangent bundle $T\mathcal{M}$ is a smooth map $s : \mathcal{M} \to T\mathcal{M}$, such that $\pi \circ s = id_{\mathcal{M}}$. A vector field on $\mathcal{M}$ is a smooth section of the tangent bundle $T\mathcal{M}$.*

If a section is only defined within a coordinate chart, then the section is called a local section. In general, a tensor field of type (p, q) is a smooth section S of the tensor product bundle $\otimes^p T\mathcal{M} \otimes^q T^*\mathcal{M}$ with components $S^{\mu_1 \cdots \mu_p}_{\nu_1 \cdots \nu_q}$.

We now define what a fibre bundle is.

Definition 2.1.18 *A fibre bundle $(E, \pi, \mathcal{M}, F, G)$ has the following elements:*

(i) It has a differentiable manifold E called the total space.

(ii) It has a differentiable manifold $\mathcal{M}$ called the base space.

(iii) It has a differentiable manifold F called the fibre.

(iv) It has a surjection map $\pi : E \to \mathcal{M}$ called the projection. The inverse image of projection at point p is called the fibre at p.

(v) It has a Lie group G, acting on the left of F, called the structure group.

A fibre bundle is often denoted by $E \xrightarrow{\pi} \mathcal{M}$ or simply just E.

Definition 2.1.19 *A coordinate bundle defined on U_i has two more elements:*

(i) On U_i, it has a map $\varphi_i : U_i \times F \to \pi^{-1}(U_i)$ called the local trivialisation.

(ii) On $U_i \cap U_j \neq \emptyset$, it has transition functions t_{ij}, (i.e. $\varphi_j(p, f) = \varphi_i(p, t_{ij}(p)f)$), and is invertible.

One may construct many coordinate bundles on the base space $\mathcal{M}$ with different choices of transition functions. A fibre bundle is an equivalence class of these coordinate bundles. If all transition functions t_{ij} on a fibre bundle equal to the identity map, then we call it the trivial bundle, which is a direct product, $\mathcal{M} \times F$.

Definition 2.1.20 *A fibre bundle $E \xrightarrow{\pi} \mathcal{M}$ is called a vector bundle if its fibre is a vector space. A line bundle is a vector bundle whose fibre is one-dimensional.*

We are now ready to extend all these concepts to complex manifolds.

Definition 2.1.21 *Consider complex manifolds $\mathcal{M}$ and E, and a holomorphic map π. A vector bundle $E \xrightarrow{\pi} \mathcal{M}$ with fibre $\mathbb{C}^k$ is called a holomorphic vector bundle of rank-k if its local trivialisation $\varphi_i : U_i \times \mathbb{C}^k \to \pi^{-1}(U_i)$ is a biholomorphic map.*

The simplest example of a holomorphic vector bundle is $\mathcal{M} \times \mathbb{C}^k$, which is the trivial vector bundle over $\mathcal{M}$. Another example of a holomorphic vector bundle is the holomorphic tangent bundles formed by (2.21). If the fibre is $\mathbb{C}$ (i.e. holomorphic vector bundle of rank-1), we call it the holomorphic line bundle or sometimes the canonical bundle. Note that a canonical bundle is a complex vector bundle of rank $(m, 0)$ with sections being holomorphic m-forms. On $\mathbb{CP}^N$, it is useful to remember the sections of the holomorphic line bundle are its homogeneous coordinates.

Let us use these definitions to study Chern classes. The goal is to introduce Chern classes and their properties to aid us in constructing CY manifolds. Detailed derivations of these properties might not be given as it is not our primary concern.

2.1.8 Chern Classes

The Chern class is a characteristic class that concerns the classification of the fibre bundles and measures its non-triviality. It is also a topological invariant.

Definition 2.1.22 *Let E be a complex vector bundle over a manifold $\mathcal{M}$, $\mathcal{F}$ be the curvature two-form of a connection $\mathcal{A}$ on E. The total Chern class of E, $c(E)$ is*

$$c(E) = \det(1 + \frac{i}{2\pi}\mathcal{F}). \tag{2.92}$$

The total Chern class can be written as the sum of forms of even degrees since $\mathcal{F}$ is a two-form. We can expand the total Chern class,

$$c(E) = 1 + c_1(E) + c_2(E) + \dots \tag{2.93}$$

where $c_k(E) \in H^{2k}(\mathcal{M}, \mathbb{R})$ are called the k-th Chern classes, and H denotes the cohomology group. To be pedantic, $c_k(E)$ in (2.93) are closed $2k$-forms called the Chern forms. The Chern classes are the cohomology classes of the Chern forms, and the Chern forms here are representatives of the Chern classes.

Chern classes do not depend on the choice of the connection despite the curvature two-form does. However, choosing a different connection changes the representative of the Chern classes. On a m-dimensional manifold, Chern classes $c_j(E)$ contain $2j$-forms and thus vanishes if $2j > m$. Regardless of the dimension of the manifold, Chern classes $c_j(E)$ vanishes for $j > k$ where k is the rank of the bundle E.

An explicit derivation for the Chern classes is given in [18]. By expanding the determinant, one finds

$$c_0(E) = [1] \tag{2.94}$$

$$c_1(E) = \left[\frac{i}{2\pi}\operatorname{Tr}\mathcal{F}\right] \tag{2.95}$$

$$c_2(E) = \left[\frac{1}{2}(\frac{i}{2\pi})^2(\operatorname{Tr}\mathcal{F}\wedge\operatorname{Tr}\mathcal{F} - \operatorname{Tr}(\mathcal{F}\wedge\mathcal{F}))\right] \tag{2.96}$$

$$\vdots \tag{2.97}$$

$$c_k(E) = \left[(\frac{i}{2\pi})^k \det\mathcal{F}\right] \tag{2.98}$$

For a holomorphic tangent bundle, let us denote the k-th Chern class as c_k. Our primary focus is the Chern classes on Kähler manifolds, especially the first Chern class. On a holomorphic tangent bundle, $\mathcal{F} = -i\mathcal{R}$, and thus $c_1 = [\operatorname{Tr}\mathcal{R}/2\pi]$, which is compatible with what we have previously defined in ch 2.1.5. Thus, the first Chern class vanishes if the Kähler metric is Ricci flat.

This is where the famous Calabi conjecture enters. He believes there exists a unique Ricci-flat metric on a Kähler manifold if it has a vanishing first Chern class. Calabi proved the uniqueness of such metric if it exists, and later Yau proved its existence. Kähler manifolds with vanishing c_1 are called Calabi-Yau manifolds, which have a great impact on string theory. A much more detailed discussion on the Calabi-Yau manifolds will be given in later chapters.

Let us define some useful properties of Chern classes for later calculations. We first introduce the notion of an exact sequence.

Definition 2.1.23 *An exact sequence is a sequence of spaces and maps,*

$$A_1 \xrightarrow{a_1} A_2 \xrightarrow{a_2} \ldots \xrightarrow{a_k} A_{k+1} \tag{2.99}$$

such that $\operatorname{Im}(a_k) = \ker(a_{k+1})$ *for all* k.

A short exact sequence is an exact sequence that takes the following form,

$$0 \xrightarrow{a} A \xrightarrow{b} B \xrightarrow{c} C \xrightarrow{d} 0 \tag{2.100}$$

where 0 is the trivial vector space.

The short exact sequence implies $c(B) = c(A)c(C)$. We can interpret (2.100) as

$A \subseteq B$ and $C = B/A$. Consider a direct sum bundle $V = E \oplus F$. Following the properties of the determinant, we have $c(V) = c(E) \wedge c(F)$. This also implies the short exact sequence $0 \to E \to V \to F \to 0$ holds.

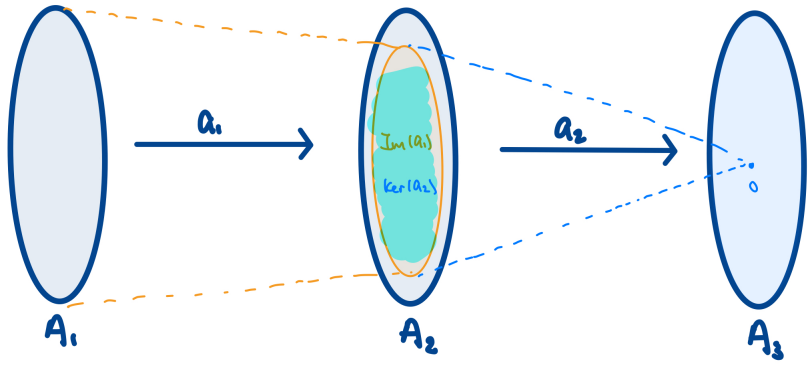

Figure 2.1: Illustration of the condition $\mathrm{Im}(a_k) = \ker(a_{k+1})$.

Another useful quantity related to Chern classes is the Chern character.

Definition 2.1.24 *The total Chern character is defined*

$$\mathrm{ch}(E) = \mathrm{Tr} \exp\left(\frac{i}{2\pi}\mathcal{F}\right) = \sum_{j=1} \frac{1}{j!} \mathrm{Tr}\left(\frac{i}{2\pi}\mathcal{F}\right)^j. \tag{2.101}$$

The j-th Chern character is defined

$$\mathrm{ch}_j(E) = \frac{1}{j!} \mathrm{Tr}\left(\frac{i}{2\pi}\mathcal{F}\right)^j. \tag{2.102}$$

On m-dimensional base space with rank-k bundle E, $\mathrm{ch}_j(E)$ with $2j > m$ vanishes. Thus, $\mathrm{ch}(E)$ is a finite order polynomial. If we diagonalise $\mathcal{F}$, such that

$$\frac{i}{2\pi}\mathcal{F} \to g^{-1}\left(\frac{i}{2\pi}\mathcal{F}\right)g = A \equiv \mathrm{diag}(x_1, \ldots, x_k) \tag{2.103}$$

where $g \in \mathrm{GL}(k, \mathbb{C})$, we find the total Chern character,

$$\mathrm{ch}(E) = \mathrm{Tr} \exp A = \sum_{j=1}^{k} \exp x_j \tag{2.104}$$

$$= k + c_1(E) + \frac{1}{2!}(c_1(E)^2 - 2c_2(E)) + \ldots. \tag{2.105}$$

Alternatively, one can write the total Chern class as $c(E) = \prod_{j=1}^{k}(1 + x_j)$ which gives the same total Chern character as in (2.104). Notice that x_j defines the

Chern classes intrinsically. Some useful identities, $\mathrm{ch}(E \oplus F) = \mathrm{ch}(E) + \mathrm{ch}(F)$ and $\mathrm{ch}(E \otimes F) = \mathrm{ch}(E)\,\mathrm{ch}(F)$.

A final useful equation to be mentioned is the relation between Chern classes and the Euler characteristic. Consider a holomorphic tangent bundle on m-dimensional manifold $\mathcal{M}$, $T^{(1,0)}\mathcal{M}$. The Euler characteristic of $\mathcal{M}$,

$$\chi = \int_{\mathcal{M}} c_m(\mathcal{M}) \tag{2.106}$$

is the integral of the top Chern class over the manifold $\mathcal{M}$. See [20, 25] for a detailed discussion.

Example: Chern classes of $\mathbb{CP}^N$

Recall the homogeneous coordinates z^m on $\mathbb{C}^{N+1}$ are sections of the holomorphic line bundle, L. Denote s_i as sections of L, $s_i \in \mathcal{O}_{\mathbb{CP}^N}(1)$, we have $s_i(z)\frac{\partial}{\partial z_i}$ spanning both the holomorphic tangent bundle $T^{(1,0)}\mathbb{C}^{N+1}$ and the holomorphic tangent bundle $T^{(1,0)}\mathbb{CP}^N$. However one has to take into account for trivial overall rescaling in $\mathbb{CP}^N$. This implies a map from the direct sum, $\mathcal{O}_{\mathbb{CP}^N}(1)^{\oplus(N+1)}$, to $T^{(1,0)}\mathbb{CP}^N$ with kernel being the trivial line bundle $\mathbb{C}$. Thus, we have a short exact sequence,

$$0 \to \mathbb{C} \to \mathcal{O}_{\mathbb{CP}^N}(1)^{\oplus(N+1)} \to T^{(1,0)}\mathbb{CP}^N \to 0. \tag{2.107}$$

From the sequence, we have $c(\mathcal{O}_{\mathbb{CP}^N}(1)^{\oplus(N+1)}) = c(\mathbb{C})c(T^{(1,0)}\mathbb{CP}^N)$. Obviously, $c(\mathbb{C}) = 1$. By the properties of Chern classes, we have

$$c(\mathbb{CP}^N) = c(T^{(1,0)}\mathbb{CP}^N), \quad c(\mathcal{O}_{\mathbb{CP}^N}(1)^{\oplus(N+1)}) = \left[c(\mathcal{O}_{\mathbb{CP}}(1))\right]^{N+1}. \tag{2.108}$$

Since $\mathcal{O}_{\mathbb{CP}}(1)$ is a line bundle, its Chern classes c_j terminates for $j \geq 2$. Expanding the total Chern class, we find $c(\mathcal{O}_{\mathbb{CP}}(1)) = 1 + c_1(\mathcal{O}_{\mathbb{CP}}(1))$.

Let $x = c_1(\mathcal{O}_{\mathbb{CP}}(1))$, we conclude the total Chern class for $\mathbb{CP}^N$,

$$c(\mathbb{CP}^N) = (1 + x)^{N+1}. \tag{2.109}$$

3 Calabi-Yau Manifolds

In the 1950s, Calabi gave his famous conjecture [3].

Conjecture 3.0.1 (Calabi) *Let $\mathcal{M}$ be a compact Kähler manifold with Kähler metric g and Kähler form w. Let $\mathcal{R}$ be the Ricci-form associated with the metric g, and represents the first Chern class $c_1(\mathcal{M})$. Then there exists a unique Kähler metric $\tilde{g}$ with Kähler form $\tilde{w}$, such that it is cohomologous to the original metric g, $[w] = [\tilde{w}]$, and whose Ricci form is $\mathcal{R}$.*

The conjecture gives a link between geometry and topology and has a far-reaching impact on both string theory and mathematics. Calabi proved the uniqueness of $(\tilde{g}, \tilde{w})$ and Yau proved its existence [4]. Therefore, if $c_1 = 0$ on a Kähler manifold, the Calabi conjecture with Yau's theorem guarantees the existence of a unique Ricci-flat Kähler metric in each Kähler class on a Calabi-Yau manifold.

Definition 3.0.1 *A m-dimensional Calabi-Yau manifold is a m-dimensional compact Kähler manifold with the following properties:*

(i) has zero Ricci-form.

(ii) has vanishing first Chern class, $c_1 = 0$.

(iii) has honolomy $\mathrm{Hol}(g) \subseteq \mathrm{SU}(m)$.

(iv) admits a globally defined and nowhere vanishing holomorphic m-form.

The emergence of Calabi-Yau manifolds initiated a series of intensive studies in string theories and led to the discovery of mirror symmetry which has great implications in both string theory and mathematics. Our primary focus is on studying ways of constructing Calabi-Yau manifolds for superstring compactification. Then, we will briefly mention what Calabi-Yau moduli space mean to string theory and to

the study of numerical Calabi-Yau metrics. Let us first motivate the study of the Calabi-Yau manifold through string theory in the next chapter, then we explain the origin of property (iv) from definition 3.0.1.

3.1 Significance in Physics

Superstring theory is directly formulated in ten spacetime dimensions. For it to make contact with our physical world, it is obvious that the low energy limit of the solution of the theory should be a 4-dimensional effective field theory (EFT), which contains our Standard Model and is coupled to Einstein's general relativity.

To find our desired solution, one can use the standard technique called compactification. We start by postulating the underlying 10-dimensional manifold M_{10} as a product manifold of a 4-dimensional Minkowski space M_4 with a 6-dimensional compact and small Riemannian manifold M_6. We call M_6 the internal space. A 4-dimensional EFT arises from averaging the low energy physics over M_6, and thus the physics of the EFT depends on the choice of the internal space. Since we wanted our space to admit solutions to Einstein's field equation, we require the Ricci tensor of M_6 to satisfy the vacuum equation. Hence, M_6 must admit a Ricci-flat metric.

Let us illustrate the above concretely. Consider $M_{10} = M_6 \times M_4$, such that M_4 has a Minkowski metric $\eta_{\mu\nu}$ and M_6 has a metric g_{ij}. We restrict the theory on M_{10} to satisfy Einstein's equations and preserve 4-dimensional Poincaŕe invariance. We can write the most general metric as [28],

$$G_{IJ} = \begin{pmatrix} f\eta_{\mu\nu} & 0 \\ 0 & g_{ij} \end{pmatrix} \tag{3.1}$$

where f is a real valued function on M_6 and the indices ranges $0 \leq I < 10$, $0 \leq \mu < 4$ and $1 \leq i \leq 6$. Then one finds the Einstein field equations reduce to Ricci flatness of G_{IJ}, which implies f to be constant, and g_{ij} to be Ricci-flat.

Ricci-flatness is not enough to resolve an EFT with appealing physical phenomena. In fact, we would like to seek a theory that has a low-energy supersymmetry since it addresses troubling issues, for instance, it provides an explanation for the gauge hierarchy problem. Furthermore, the EFT has to resolve the SM gauge group $SU(3) \times SU(2) \times U(1)$ in low energy limit. It was found that if the theory reproduces our observed three-generational families of leptons and quarks, then the internal space must have $\chi = \pm 6$, where χ is the Euler characteristic. A detailed discussion on these conditions is present in [29], which is beyond the scope of this dissertation. Eventually, all these conditions lead to the conclusion that the internal space should be a Calabi-Yau threefold. The first application of Calabi-Yau manifolds in string theory was carried out by Candelas, Horowitz, Strominger, and Witten in 1985 [2], where they showed how a compactification of heterotic $E_8 \times E_8$ strings leads to the SM.

After compactification, one can fix the particle content via the topological data of the internal space and the choice of gauge bundle V. However, there is a vast amount, around 10^6 Calabi-Yaus [8] that satisfies the condition of $\chi = \pm 6$, forming the so-called "Calabi-Yau landscape". In general, the geometry of these Calabi-Yaus are different and give rise to different EFTs, despite generating the desired particle spectrum. To test if the resulting EFT describes our universe, we need to compute the observables, such as the masses and couplings of particles, for direct comparison with experimental observations. Unfortunately, calculating these observables requires the knowledge of the Ricci-flat metric on the internal space Calabi-Yau threefold, which by date has no known analytic expressions. This calls for numerical methods which will be discussed in the next chapter.

Before moving on, let us review the $D = 5$ Kaluza-Klein theory to illustrate the idea of compactification. Such an idea is carried over to string compactification.

3.2 Kaluza-Klein Compactification

The Kaluza-Klein compactification was first introduced to unify gravity and electromagnetism via the idea of higher dimensional theory. Let us assume the background spacetime takes the form $M_4 \times S^1$ with local coordinates (x^μ, y). Consider the Einstein-Hilbert action,

$$S = \frac{1}{2\kappa^2} \int d^4x dy \sqrt{-\hat{g}} R^{(5)}, \tag{3.2}$$

where $R^{(5)}$ is the $D = 5$ Ricci scalar. The metric is given by [30],

$$\hat{g}_{MN} = \phi^{-\frac{1}{3}} \begin{pmatrix} g_{\mu\nu} + \kappa^2 \phi A_\mu A_\nu & \kappa \phi A_\mu \\ \kappa \phi A_\nu & \phi \end{pmatrix}. \tag{3.3}$$

The physical radius of S^1 can be fixed via a choice of the coordinate radius R,

$$\text{Area of } S^1 = \int_0^{2\pi R} \mathrm{d}y \phi^{\frac{1}{3}} \tag{3.4}$$

If we assume $\phi \to 1$ at spatial infinity, we find the Area of $S^1 = 2\pi R$, and thus we get R as the physical radius. Notice that if we have $\phi \to 2$ instead (i.e. changing the vev), then our physical radius becomes $2R$. We see the physical radius depends on ϕ which in turn depends on $\hat{g}_{MN}$, and nothing explicitly fixes it. Thus, we have a one-parameter moduli space, where R serves as the parameter.

On the circle with R being the physical radius, any fields on this $D = 5$ space-time has periodic boundary conditions, i.e. $\phi(x^\mu, y) = \phi(x^\mu, y + 2\pi R)$. This allows a Fourier expansion in terms of the eigenfunctions of the circle,

$$\phi(x^\mu, y) = \sum_n \phi_n(x) e^{iny/R}$$

$$A_\mu(x^\mu, y) = \sum_n A_{\mu n}(x) e^{iny/R}, \quad g_{\mu\nu}(x^\mu, y) = \sum_n g_{\mu\nu n}(x) e^{iny/R}.$$

Examining the Klein-Gordan equation,

$$\hat{\Box}\phi(x^\mu, y) = 0 \quad \Rightarrow \quad \left[\Box + \partial_y^2\right] \phi_n(x) \equiv \left[\Box + (\frac{n}{R})^2\right] \phi_n(x) = 0 \tag{3.5}$$

we have an infinite number of ϕ_n called the massive Kaluza-Klein (KK) modes with mass $M = |\frac{n}{R}|$. Compactification is done by taking the limit $R \to 0$, which results in infinitely massive KK modes. In a low-energy EFT, we can ignore all these infinitely massive modes but keep only the $n = 0$ massless mode. This eliminates all y-dependencies and yields a 4d EFT,

$$S = \int d^4x\sqrt{-g}(\frac{R^{(4)}}{\kappa^2} - \frac{1}{4}\phi F_{\mu\nu}F^{\mu\nu} - \frac{1}{6\kappa^2\phi^2}\partial^\mu\phi\partial_\mu\phi), \tag{3.6}$$

where $R^{(4)}$ is the $D = 4$ Ricci scalar, and ϕ is a massless scalar which is referred to as the moduli. Since there are no massless scalar fields observed in our universe, we have to "fix" the moduli for the theory to be a working theory. This can be done by introducing mechanisms to make ϕ massive. Generally, every parameter on the moduli space gives rise to a light field in the low-energy EFT in the context of superstring compactification. Therefore, the knowledge of the moduli space is crucial.

3.3 Holomorphic volume form

Let us now show a m-dimensional Calabi-Yau manifold has a nowhere-vanishing holomorphic $(m, 0)$-form. Such a $(m, 0)$-form is sometimes called the holomorphic volume form. For our purposes, let us consider a Calabi-Yau threefold $\mathcal{M}$ and assume the existence of a holomorphic volume form,

$$\Omega = \frac{1}{3!}\Omega_{\mu\nu\rho}dx^\mu \wedge dx^\nu \wedge dx^\rho. \tag{3.7}$$

We can use Ω to define a coordinate scalar,

$$\|\Omega\|^2 = \frac{1}{3!}\Omega_{\mu\nu\rho}\bar{\Omega}^{\mu\nu\rho}. \tag{3.8}$$

Within a coordinate patch, we may write

$$\Omega_{\mu\nu\rho}(x) = f(x)\epsilon_{\mu\nu\rho} \tag{3.9}$$

where $f(x)$ is a nowhere vanishing holomorphic function. Using the Kähler metric g on the Calabi-Yau manifold, one finds the complex conjugate,

$$\bar{\Omega}^{\sigma\lambda\tau} = \bar{f}\epsilon_{\bar{\mu}\bar{\nu}\bar{\rho}}g^{\sigma\bar{\mu}}g^{\lambda\bar{\nu}}g^{\tau\bar{\rho}} = g^{-\frac{1}{2}}\bar{f}\epsilon^{\sigma\lambda\tau} \tag{3.10}$$

where $g = \det(g_{mn})$. Rearrange for g, we get

$$g^{\frac{1}{2}} = \frac{|f|^2}{\|\Omega\|^2} \Rightarrow \mathcal{R} = -i\partial\bar{\partial}\log g^{\frac{1}{2}} = -i\partial\bar{\partial}\log(|f|^2) + i\partial\bar{\partial}\log(\|\Omega\|^2). \tag{3.11}$$

We see $\mathcal{R}$ is exact since $\log(\|\Omega\|^2)$ is a coordinate scalar. Thus, the cohomology class $[\mathcal{R}]$ vanishes, implying a trivial first Chern class $c_1(\mathcal{R}) = 0$.

Let us conclude the proof by showing the converse holds. There are two different approaches in showing so presented in [6]. The first approach will be shown through an example of the quintic in later chapters. We shall focus on the second approach as it is relatively intuitive. However, it applies knowledge from Čech cohomology, which we have not discussed before. For our purposes, a sketch of the proof will suffice. By Yau's theorem, we are guaranteed a metric that satisfies $\partial_\mu\partial_{\bar{\nu}}\log g^{\frac{1}{2}} = 0$. It implies that there exists a function f on the j-th coordinate patch U_j such that $g_i^{\frac{1}{2}} = |f_i|^2$. The idea of this approach is to show that we can pick a phase to construct a 3-form that is in fact equivalent to the holomorphic volume form,

$$e^{-i\theta_i}f_i(x)dx_i^1 \wedge dx_i^2 \wedge dx_i^3 \tag{3.12}$$

where θ_i is the phase, and (3.12) is independent of coordinate choice. First, consider the coordinate transformation of f_i on $U_i \cap U_j$,

$$g_i^{\frac{1}{2}}\left|\frac{\partial x_i}{\partial x_j}\right|^2 = g_j^{\frac{1}{2}} \quad \Rightarrow \quad |f_i|^2\left|\frac{\partial x_i}{\partial x_j}\right|^2 = |f_j|^2 \tag{3.13}$$

Writing all the modulus squared as $|f_i|^2 = f_i\bar{f}_i$ and rearranging the variables,

$$\frac{f_i\frac{\partial x_i}{\partial x_j}}{f_j} = \overline{(\frac{f_j}{f_i\frac{\partial x_i}{\partial x_j}})}. \tag{3.14}$$

The object to the left of the first equality is a function of x^μ, while the object to the right is a function of $x^{\bar{\mu}}$. The two objects are equal only if they are constant. Let us

write this constant as $e^{i\theta_{ij}}$, where θ_{ij} is real. Consider also the inverse transformation of f_i, we find $\theta_{ij} = -\theta_{ji}$. On $U_i \cap U_j \cap U_k$, we find $\theta_{ij} + \theta_{jk} + \theta_{ki} = 0$. The magic of Čech cohomology is that it tells us these two equations imply that θ_{ij} is a one-cochain which is also a boundary. The analogy in de Rham cohomology[1] is θ_{ij} being a one-form that is closed and exact. Consequently, we can write $\theta_{ij} = \theta_i - \theta_j$ where θ_i is some constant on U_i. Thus,

$$\frac{f_i \frac{\partial x_i}{\partial x_j}}{f_j} = e^{i\theta_{ij}} \quad \Rightarrow \quad e^{-i\theta_i} f_i \frac{\partial x_i}{\partial x_j} = e^{-i\theta_j} f_j. \tag{3.15}$$

Hence, equation (3.12) is independent of the choice of coordinates and is a globally defined and nowhere vanishing holomorphic (3,0)-form. Thus, c_1 vanishes if and only if $\mathcal{M}$ admits a nowhere vanishing holomorphic (3,0)-form, and vice versa.

3.4 The Monge-Ampére Equation

We can reformulate the Calabi conjecture into a Monge-Ampére equation of the Kähler potential. It provides a direct way to check if the Kähler potentials satisfy the Kähler condition. Recall the Ricci-tensor of a Kähler metric has expression, $R_{\mu\bar{\nu}} = -\partial_\mu \partial_{\bar{\nu}} \log \det g_{\mu\bar{\nu}}$. The Einstein equation implies $\partial_\mu \partial_{\bar{\nu}} \log \det g_{\mu\bar{\nu}} = 0$, which is a fourth-order PDE in terms of the Kähler potential. However, this equation can be reduced into a second-order PDE, called the Monge-Ampére equation.

Consider Calabi-Yau threefold with the Kähler form w. Let Ω be the holomorphic volume form, which defines a volume form $\mu = (-i)^3 \Omega \wedge \bar{\Omega}$. Let us define,

$$v_w = \frac{w \wedge w \wedge w}{3! \mu} = \frac{(i)^3 g_{\mu_1 \bar{\nu}_1} g_{\mu_2 \bar{\nu}_2} g_{\mu_3 \bar{\nu}_3} dz^{\mu_1} \wedge dz^{\bar{\nu}_1} \wedge ... \wedge dz^{\mu 3} \wedge dz^{\bar{\nu}_3}}{3!(-i)^3 |\Omega_{\mu_1 \mu_2 \mu_3}|^2 dz^{\mu_1} \wedge ... \wedge dz^{\mu_3} \wedge dz^{\bar{\mu}_1} \wedge ... \wedge dz^{\bar{\mu}_3}} \tag{3.16}$$

$$= \frac{\det g_{\mu\bar{\nu}}}{|\Omega_{123}|^2}. \tag{3.17}$$

One can check, with the use of the Einstein equations,

$$-\partial_\mu \partial_{\bar{\nu}} \log v_w = -\partial_\mu \partial_{\bar{\nu}} \log \det g_{\mu\bar{\nu}} + \partial_\mu \partial_{\bar{\nu}} \log |\Omega_{123}|^2 = 0 \tag{3.18}$$

[1] Čech cohomology is equivalent to de Rham cohomology if the betti number $b_1 = 2b_{10} = 0$. This is satisfied on a Calabi-Yau manifold with a non-zero Euler number.

where the last term vanishes as $\partial_\mu \bar{\Omega}_{123} = \partial_{\bar{\mu}} \Omega_{123} = 0$. Hence, on Calabi-Yau manifolds, $v_w = \textit{constant}$ is equivalent to satisfying the Monge-Ampere equation.

To illustrate the idea concretely, let us try to recast the Calabi conjecture into a Monge-Ampere equation. We have a Ricci-flat metric in every Kähler class on the Calabi-Yau manifold, X. Let R_{CY} be the Ricci form corresponding to the Ricci-flat metric g_{CY}. Let $\tilde{R}$ be another Ricci form whose metric $\tilde{g}$ is in the same Kähler class with g_{CY}, i.e. $g_{CY} = \tilde{g} + \partial\bar{\partial}\phi$ for some scalar function ϕ. Since c_1 vanishes, we can write $R_{CY} = \tilde{R} + \partial\bar{\partial}F$, where $\partial\bar{\partial}F$ is some exact form. Rearranging,

$$\partial_i \partial_{\bar{j}} \log\det g_{CY} = \partial_i \partial_{\bar{j}} \log\det \tilde{g} + \partial_i \partial_{\bar{j}} F \tag{3.19}$$

$$\partial_i \partial_{\bar{j}} [\log\det(\tilde{g} + \partial\bar{\partial}\phi) - \log(\det \tilde{g} \cdot e^F)] = 0 \tag{3.20}$$

$$\partial_i \partial_{\bar{j}} [\log(\det(\tilde{g} + \partial\bar{\partial}\phi) \cdot (\det \tilde{g} \cdot e^F)^{-1})] = 0 \tag{3.21}$$

$$\log(\det(\tilde{g} + \partial\bar{\partial}\phi) \cdot (\det \tilde{g})^{-1} e^{-F})) = C \tag{3.22}$$

where C is a constant, and we have used the maximum principle on a compact manifold at (3.21). Assuming $\int_X e^F = \mathrm{Vol}(X)$, we have the condition $C = 0$. Thus, we have the Monge-Ampére equation, $\det(\tilde{g} + \partial\bar{\partial}\phi) = (\det \tilde{g}) e^F$. If there exists a ϕ that satisfies this equation, then g_{CY} is proven to be the Calabi-Yau metric. This is the setup of how Yau proved Calabi's conjecture.

3.5 Construction of Calabi-Yau Manifolds

There are numerous ways of constructing a Calabi-Yau manifold. Perhaps, the simplest method is to construct it as a hypersurface in projective spaces. The merit of constructing a Calabi-Yau as a submanifold of projective space is that projective space guarantees its submanifold being compact and Kähler, see the example given in chapter 2. Let us start by stating a useful theorem by Chow,

Theorem 3.5.1 (chow) *Analytic submanifolds of projective spaces may be realised as the zero locus of a finite number of polynomials of homogeneous coordinates. We*

call such submanifolds as algebraic variety.

This allows us to construct a Calabi-Yau manifold as a complete intersection submanifold. Let us clarify what we mean. We aim to construct Calabi-Yaus as submanifold $\mathcal{M}$ in a product of projective spaces of total dimension $N+3$, such that $\mathcal{M}$ are complete intersections of N polynomials p^α, $\alpha = 1, ..., N$. The condition for the submanifold being a complete intersection is that the N-form on $\mathcal{M}$,

$$\Psi = dp^1 \wedge dp^2 \wedge \cdots \wedge dp^N \tag{3.23}$$

is nowhere vanishing, which implies $\mathcal{M}$ being smooth. If Ψ vanishes at a point $p \in \mathcal{M}$, we then have at least one of the dp^i vanishes and thus does not have well defined normal directions at p, which implies $\mathcal{M}$ cannot be smooth. Notice that, choosing N polynomials in the $N+3$ dimensional space gives locally a 3-dimensional manifold, which is desired for our compactification space.

By Chow's theorem, the submanifold $\mathcal{M}$ is compact and Kähler. If $\mathcal{M}$ is a Calabi-Yau manifold, then its first Chern class has to vanish. We should examine what restrictions can be imposed on the polynomials to obtain $c_1 = 0$ on $\mathcal{M}$. As shown in the previous chapter, the first Chern class vanishes if $\mathcal{M}$ admits a nowhere vanishing holomorphic volume form. We can use this to impose the necessary conditions on the polynomials, as shown in [6]. However, let us use another approach that employs the use of the Chern character and Chern classes.

The goal is to compute the first Chern class and see under what conditions it vanishes. For starters, let us consider constructing a Calabi-Yau on one projective space instead of complete intersections. Let X be an analytic submanifold, explicitly a smooth hypersurface, in $\mathbb{CP}^N$. By Chow's theorem, X is realised as the zero-locus of a degree d polynomial, p (p is a section of the holomorphic line bundle $\mathcal{O}_{\mathbb{CP}^N}(d)$). We can define the normal bundle N_X of X as the quotient

$$N_X = \frac{T^{(1,0)}\mathbb{CP}^N|_X}{T^{(1,0)}X} \tag{3.24}$$

where $T^{(1,0)}X$ is the holomorphic tangent bundle of X. From (2.100), we have a short exact sequence, $0 \to T^{(1,0)}X \to T^{(1,0)}\mathbb{CP}^N|_X \to N_X \to 0$. In fact, p serves as a coordinate near X, and thus the normal bundle is simply the holomorphic line bundle $\mathcal{O}_{\mathbb{CP}^N}(d)|_X$. Our short exact sequence becomes,

$$0 \to T^{(1,0)}X \to T^{(1,0)}\mathbb{CP}^N|_X \to \mathcal{O}_{\mathbb{CP}^N}(d)|_X \to 0 \tag{3.25}$$

which is called the adjunction formula (see more in [31]). The short exact sequence implies $c(X) = c(\mathbb{CP}^N)/c(\mathcal{O}_{\mathbb{CP}^N}(d))$. Since $\mathcal{O}_{\mathbb{CP}^N}(d)$ is a line bundle, we have $c_j(\mathcal{O}_{\mathbb{CP}^N}(d)) = 0$ for $j \geq 2$. The Chern character,

$$ch(\mathcal{O}_{\mathbb{CP}^N}(d)) = e^{dx} = 1 + dx + \cdots = 1 + c_1(\mathcal{O}_{\mathbb{CP}^N}(d)) + \cdots \Rightarrow c_1 = dx. \tag{3.26}$$

Hence, the total Chern class $c(\mathcal{O}_{\mathbb{CP}^N}(d)) = 1 + c_1 = 1 + dx$. Recall from the end of the previous chapter, we have $c(\mathbb{CP}^N) = (1+x)^{N+1}$. Together,

$$c(X) = \frac{(1+x)^{N+1}}{1+dx}. \tag{3.27}$$

By definition, x is a closed two-form. We can expand the total Chern class as wedge products of x and extract the first Chern class,

$$c(X) = (1 + (N+1)x + \dots)(1 - dx + \dots) = 1 + [(N+1) - d]x + \dots. \tag{3.28}$$

We find the first Chern class being

$$c_1(X) = [(N+1) - d]x. \tag{3.29}$$

If X is a Calabi-Yau threefold (i.e. $N = 4$), we require X to be the zero-locus of a degree 5 polynomial of homogeneous coordinates z. This is the well-known Fermat quintic in $\mathbb{CP}^4$. We can generalise the above results to the complete intersection manifolds Y, constructed from N degree d_i, $i = 1, ..., N$, polynomials,

$$c(Y) = \frac{(1+x)^{N+1}}{\prod_{i=1}^{l}(1+d_i x)}. \tag{3.30}$$

If $c_1(Y) = 0$, we have the condition $N + 1 = \sum_{i=1}^{l} d_i$.

Example: The Fermat Quintic

The quintic threefold is perhaps the most studied Calabi-Yau manifold in the context of numerical Calabi-Yau metrics. It is a 3-dimensional hypersurface defined by a degree-5 homogeneous polynomial in the 4-dimensional complex projective space $\mathbb{CP}^4$. We can find $\binom{5+5-1}{5-1} = 126$ independent polynomials that satisfy the quintic polynomial condition. However, the symmetries on $\mathbb{CP}^4$, see Chapter 4.2, finds 25 of them redundant. Thus, there are 101 independent polynomials that define the quintic. The simplest example of the quintic is the Fermat quintic, defined by,

$$Q(z) = \sum_{i=1}^{5} (z_i)^5 = (z_1)^5 + (z_2)^5 + (z_3)^5 + (z_4)^5 + (z_5)^5 = 0, \tag{3.31}$$

where $z^i \in \mathbb{C}^5$ are the homogeneous coordinates of $\mathbb{CP}^4$.

Let us try to find the holomorphic volume form Ω on Q. On $\mathbb{C}^5$, we define

$$\tau = \epsilon_{a_1 \ldots a_5} z^{a_1} dz^{a_2} \wedge dz^{a_3} \wedge \ldots \wedge dz^{a_5} = \sum_{\mu=1}^{5} dz_1 \wedge \ldots \wedge z_\mu \wedge \ldots \wedge dz_5 \tag{3.32}$$

which is clearly a holomorphic (4,0)-form. However, τ is not well defined on $\mathbb{CP}^4$ since it transforms as $\tau \to \lambda^5 \tau$ under the transformation $z^a \to \lambda z^a$. Instead, we find τ/Q, which has poles at $Q = 0$, being invariant under the transformation $z^a \to \lambda z^a$. Let γ_Q be a small circle of radius δ around $Q = 0$ in $\mathbb{CP}^4$. Let us define the holomorphic, nowhere vanishing $(3,0)$-form Ω via,

$$\lim_{\delta \to 0} \int_{\gamma_Q} \frac{\tau}{Q} = (2\pi i)\Omega. \tag{3.33}$$

By rewriting dz_1 as $dz_1 = (\frac{\partial z_1}{\partial Q}) dQ$, and evaluate the integral, we find

$$\Omega = \left(\frac{\sum_{\mu=2}^{5} dz_2 \wedge \ldots \wedge z_\mu \wedge \ldots \wedge dz_5}{(\partial Q / \partial z_1)} \right) \Bigg|_{Q=0}. \tag{3.34}$$

where $(2\pi i)$ from (3.33) cancels due to the residue theorem. The existence of such a nowhere-vanishing holomorphic volume form concludes that the quintic is indeed a Calabi-Yau manifold, verifying our condition achieved previously via the computation of the first Chern class.

It is worth mentioning another family of quintic threefold, the Dwork family: $Q(z) = \sum_{i=1}^{5}(z_i)^5 - 5\psi\prod_{i=1}^{5} z_i = 0$ has an interesting relation to mirror symmetry.

3.6 Moduli spaces

There are two important moduli spaces for a Calabi-Yau manifold, that is the complex structure moduli and the Kähler moduli. These moduli determine the geometry of the Calabi-Yau manifold and thus determine string phenomenology. For instance, the shape and size of a Calabi-Yau depend on its complex structure and Kähler moduli respectively, which in turn determines some physical quantity of the theory, such as the gauge group and the particle content.

Let us start with the complex structure moduli. The space of complex structure of a Calabi-Yau manifold is called the Calabi-Yau moduli space. To illustrate the idea, consider the torus[2]. A complex torus, $\mathbb{C}/L(\lambda_1, \lambda_2)$ can be formed under the identification $z \sim z + m\lambda_1 + n\lambda_2$ for fixed non-zero λ_1, λ_2, such that, $\mathrm{Im}(\lambda_1/\lambda_2) > 0$, $\lambda_1/\lambda_2 \notin \mathbb{R}$ with $m, n \in \mathbb{Z}$. Complex coordinates on T^2 is fixed by choosing a pair of (λ_1, λ_2), hence, we say the complex structure of T^2 is defined by the pair (λ_1, λ_2). The lattice $L(\lambda_1, \lambda_2) \equiv \{\lambda_1 m + \lambda_2 n | m, n \in \mathbb{Z}\}$ on T^2 is not uniquely determined by (λ_1, λ_2). Two lattices $L(\lambda_1, \lambda_2)$ and $L'(\lambda_1', \lambda_2')$ coincides if

$$\begin{pmatrix} \lambda_1' \\ \lambda_2' \end{pmatrix} = \begin{pmatrix} a & b \\ c & d \end{pmatrix} \begin{pmatrix} \lambda_1 \\ \lambda_2 \end{pmatrix} \equiv A \begin{pmatrix} \lambda_1 \\ \lambda_2 \end{pmatrix} \tag{3.35}$$

such that $A \in \mathrm{PSL}(2, \mathbb{Z}) \equiv \mathrm{SL}(2, \mathbb{Z})/\mathbb{Z}^2$ (One can check A and $-A$ defines the same lattice). It implies (λ_1, λ_2) and (λ_1', λ_2') defines the same complex structure.

Let us define the two projection maps $p : \mathbb{C} \to \mathbb{C}/L(\lambda_1, \lambda_2)$, $\tilde{p} : \mathbb{C} \to \mathbb{C}/L(\lambda_1', \lambda_2')$ and assume the exsistence of a one-to-one holomorphic map, $h : \mathbb{C}/L(\lambda_1, \lambda_2) \to \mathbb{C}/L(\lambda_1', \lambda_2')$. It induces a holomorphic map h_* between the two $\mathbb{C}$. In fact, we have

[2]Torus is the only compact Calabi-Yau manifold in one-dimension.

the commutative diagram

$$\begin{array}{ccc} \mathbb{C} & \xrightarrow{\quad h_* \quad} & \mathbb{C} \\ \Big\downarrow{\scriptstyle p} & & \Big\downarrow{\scriptstyle \tilde{p}} \\ \mathbb{C}/L(\lambda_1,\lambda_2) & \xrightarrow{\quad h \quad} & \mathbb{C}/L(\lambda_1',\lambda_2') \end{array} \tag{3.36}$$

such that $\tilde{p} \circ h_*(z) = h \circ p(z), \forall z \in \mathbb{C}$. The induced map must take the form $z \to h_*(z) = az + b$, where $a, b \in \mathbb{C}$ and $a \neq 0$. Clearly, $h_*(\lambda_1) - h_*(0) = a\lambda_1$ and $h_*(\lambda_2) - h_*(0) = a\lambda_2$. For h to be a well defined map, we require $a\lambda_1, a\lambda_2 \in L(\lambda_1', \lambda_2')$ and $a'\lambda_1', a'\lambda_2' \in L(\lambda_1, \lambda_2)$, where $a' \neq 0 \in \mathbb{C}$. Thus, if $\mathbb{C}/L(\lambda_1,\lambda_2)$ and $\mathbb{C}/L(\lambda_1',\lambda_2')$ has the same complex structure, we must have a matrix $M \in \mathrm{SL}(2,\mathbb{Z})$ and a complex number $w = a'^{-1}$ such that

$$\begin{pmatrix} a'\lambda_1' \\ a'\lambda_2' \end{pmatrix} = M \begin{pmatrix} \lambda_1 \\ \lambda_2 \end{pmatrix} \Rightarrow \begin{pmatrix} \lambda_1' \\ \lambda_2' \end{pmatrix} = \omega M \begin{pmatrix} \lambda_1 \\ \lambda_2 \end{pmatrix}. \tag{3.37}$$

This is equivalent to saying the complex structure of (λ_1', λ_2') is defined by the pair (λ_1, λ_2) modulo a constant factor ω and $\mathrm{PSL}(2,\mathbb{Z})$.

Let us try to remove the constant factor dependence. If we define a complex-analytic isomorphism $z \to v = z/\lambda_2$, then every torus is isomorphic to one with $\lambda_2 = 1$. Let $\tau = \lambda_1/\lambda_2 \in H \equiv \{z \in \mathbb{C} | \mathrm{Im}(z) > 0\}$ be the modular parameter, and take $(\tau, 1)$ to generate a lattice. If τ and τ' defines the same complex structure, we have

$$\begin{pmatrix} \lambda_1' \\ \lambda_2' \end{pmatrix} = \begin{pmatrix} a & b \\ c & d \end{pmatrix} \begin{pmatrix} \tau \\ 1 \end{pmatrix} \Rightarrow \tau' = \frac{\lambda_1'}{\lambda_2'} = \frac{a\tau + b}{c\tau + d} \tag{3.38}$$

where $\left(\begin{smallmatrix} a & b \\ c & d \end{smallmatrix}\right) \in \mathrm{SL}(2,\mathbb{Z})$. The map $\tau' \to \tau$ is called a modular transformation, which can be generated by $\tau \to \tau + 1$ and $\tau \to -1/\tau$. The moduli space of the torus is the quotient space $H/\mathrm{PSL}(2,\mathbb{Z})$, while parameter τ defines a coordinate for the complex structure moduli. By varying τ, we vary the shape of the torus. We can interpret the moduli space as the space of parameters that describe the same object.

Let us turn to the Kähler moduli space. In essence, the space of Kähler classes is

called the Kähler moduli. Recall the set of Kähler forms w defines the Kähler class $[w] \in H^{(1,1)}(\mathcal{M})$. A Kähler class is fixed if different Kähler forms differ by an exact form $i\partial\bar{\partial}\phi$, where ϕ is a globally defined scalar, i.e. $w' = w + i\partial\bar{\partial}\phi$. Rewriting the Kähler forms in terms of Kähler potentials, we find

$$i\partial\bar{\partial}\mathcal{K}' = i\partial\bar{\partial}\mathcal{K} + i\partial\bar{\partial}\phi \quad \Rightarrow \quad \mathcal{K}' = \mathcal{K} + \phi \tag{3.39}$$

which implies that Kähler class and thus Kähler moduli can be fixed by fixing Kähler transformations. In literature, the Kähler moduli is often defined as the Kähler cone, which is the set of possible Kähler classes in $H^{(1,1)}$ that have at least one positive form. Note that the boundary of the cone represents submanifolds with zero volume. Moreover, there is a theorem, which states the Kähler cone is isomorphic to the space of Ricci-flat Kähler metrics of dimension $h^{(1,1)}$. See Chapter 5 of [32] for proof. This tells us the moduli spaces are closely related to the Hodge numbers.

Take the Dwork family as an example. The parameter ψ defines a Kähler modulus which measures the volume of the manifold. Notice that $\psi = 0$ yields the Fermat quintic. Consider the Hodge diamond of quintic threefold (see [20] for derivation),

$$\begin{array}{ccccccc}
 & & & 1 & & & \\
 & & 0 & & 0 & & \\
 & 0 & & 1 & & 0 & \\
1 & & 101 & & 101 & & 1 \\
 & 0 & & 1 & & 0 & \\
 & & 0 & & 0 & & \\
 & & & 1 & & &
\end{array}$$

Since $h^{(1,1)} = 1$, we know there is only one Ricci-flat Kähler form on the quintic and the Kähler cone is one-dimensional. Indeed, our Kähler moduli has only ψ as the parameter, making it one-dimensional. Furthermore, $h^{(2,1)} = 101$ tells us the number of complex structures we have on the quintic. This is compatible with our previous calculation on the number of independent quintic polynomials. Thus, our complex structure moduli is 101-dimensional.

Formally, $h^{(1,1)}$ and $h^{(2,1)}$ classifies the infinitesimal deformation of the Kähler moduli and the complex moduli respectively, see ch6 of [25]. A profound feature of Calabi-Yau manifolds is that they have a mirror manifold, and the pair of Calabi-Yau leads to the same worldsheet theory. This leads to the notion of mirror symmetry. Remarkably, the Hodge numbers of the pair of Calabi-Yau can be mapped to each other (i.e. $h^{(p,q)}$ and $h^{(d-p,q)}$, where d is the complex dimension of the Calabi-Yau). Taking the quintic as an example, there is a "mirror" quintic $\tilde{Q}$ with $h^{(1,1)}(\tilde{Q}) = h^{(2,1)}(Q) = 101$ and $h^{(2,1)}(\tilde{Q}) = h^{(1,1)}(Q) = 1$. In fact, lots of the properties of mirror symmetry are studied with the knowledge of the moduli spaces, which further shows the importance of moduli spaces.

4 Numerically Solving Calabi-Yau Metrics

As mentioned, there are no known analytic expressions for Calabi-Yau metrics on Calabi-Yau threefold for the time being. However, there have been plenty of efforts made in the past decade in the pursuit of a numerical Calabi-Yau metric, leading to the two best numerical algorithms in solving for Calabi-Yau metrics, that is the Donaldson algorithm and the Energy functional approach. Useful reviews of the Donaldson algorithm can be found in [17, 33], while the author of the Energy functional approach has written a user handbook [34].

4.1 Donaldson's Algorithm

Donaldson [10] pioneers the use of projective embeddings to represent a numerical metric. This idea originates from Yau and its applicability was shown by Tian [35]. This chapter introduces the algorithm and takes the quintic as an example.

Starting from a holomorphic line bundle $\mathcal{L}$ on Kähler manifold X with N global sections, we have N basis polynomials $\{s_\alpha\}_{\alpha=1}^{N}$ as the sections of the line bundle which forms the basis of the vector space $\mathrm{H}^0(X,\mathcal{L}) = \mathbb{C}^N$. Then on the bundle $\mathcal{L}^k$, we have degree-k polynomials $\{s_\alpha\}_{\alpha=1}^{N_k}$ as sections of the bundle. We will explain the k-dependence on N_k later in an example regarding the quintic. Let us construct a map, $i : X \to \mathbb{CP}^{N-1}$, such that $i(z_0, ..., z_N) = (s_1(z), ..., s_N(z))$, and require it to be an embedding[1]. The map being an embedding allows us to write the Kähler potential on X in terms of the polynomials $\{s_\alpha\}$ on $\mathbb{CP}^{N-1}$ since the coordinates on the projective space are now parametrised by the sections s_α. Here, X is embedded into $\mathbb{CP}^{N-1}$ as an algebraic variety. We now refer to the metrics and Kähler potentials on X as "algebraic metrics" and "algebraic potentials" respectively.

[1]For i to be an embedding, $\mathcal{L}$ has to be an ample line bundle

The next step is to make an ansatz for the Kähler potentials on $\mathbb{CP}^{N-1}$,

$$K_h = \frac{1}{k\pi} \ln \sum_{\alpha,\bar{\beta}=1}^{N_k} h^{\alpha\bar{\beta}} s_\alpha(x) \bar{s}_{\bar{\beta}}(\bar{x}), \tag{4.1}$$

where $h^{\alpha\bar{\beta}}$ is some invertible hermitian matrix. Notice that it has N_k^2 parameters and a form of the Fubini-Study Kähler potential which gives rise to a family of Kähler metrics on X. Note that different $h^{\alpha\bar{\beta}}$ results in different metrics but are within the same Kähler class. We compute the metric via, $g_{\alpha\bar{\beta}} = \partial_\alpha \partial_{\bar{\beta}} K_h$.

The final step is to seek which Kähler potential gives the "best" approximation to the Ricci-flat metric. Observe that (4.1) implies $h^{\alpha\bar{\beta}}$ defines a hermitian metric on $\mathcal{L}$. It allows a definition of the inner product between s_α,

$$< s_\beta | s_\alpha >= \int_X \mathrm{dVol_{CY}} \frac{s_\alpha \bar{s}_{\bar{\beta}}}{h^{\gamma\bar{\delta}} s_\gamma \bar{s}_{\bar{\delta}}}, \tag{4.2}$$

where $\mathrm{dVol_{CY}}$ is the volume form on X by choice. A typical choice for the volume form on a Calabi-Yau is $\mathrm{dVol_{CY}} = \Omega \wedge \bar{\Omega}$, where Ω is the holomorphic volume form and is independent of $h^{\alpha\bar{\beta}}$. Let us define the "T-map",

$$T : h^{\alpha\bar{\beta}} \mapsto T(h)_{\alpha\bar{\beta}} = \frac{N_k}{\mathrm{Vol_{CY}}} \int_X \mathrm{dVol_{CY}} \frac{s_\alpha \bar{s}_{\bar{\beta}}}{h^{\gamma\bar{\delta}} s_\gamma \bar{s}_{\bar{\delta}}}. \tag{4.3}$$

If h satisfies $h = T(h)$, the pair (h, s_α) is called a balanced embedding. Then the metric $g^{(k)}_{\alpha\bar{\beta}} = \partial_\alpha \partial_{\bar{\beta}} K_h$ is called the balanced metric which is unique.

Theorem 4.1.1 *If there exists a balanced embedding (h, s_α), then the sequence $T^k(h_{(0)})$ converges to a fixed point in the limit of $k \to \infty$ for any initial hermitian matrix $h_{(0)}$.*

The theorem guarantees the contraction of the T-map, and hence, iterating through the map gives us a sequence of balanced metrics. Consider the Kähler forms associated with the sequence of balanced metrics on the bundle $\mathcal{L}^k$,

$$w_k = \frac{1}{k} i_k^* (w_k^{\mathrm{FS}}) \tag{4.4}$$

where i^* denotes the pullback, and w_k^{FS} is the Kähler form with (4.1) as Kähler

potential on the projective space. It was found the Kähler class is $[w_k] = c_1(\mathcal{L})$.

Theorem 4.1.2 *If w_k converges to some limit w_∞ as $k \to \infty$, then w_∞ is a Kähler metric in the class $c_1(\mathcal{L})$ with constant scalar curvature.*

On a Calabi-Yau manifold, $c_1 = 0$ implies vanishing scalar curvature for w_k. Hence, the $k \to \infty$ limit gives us a Ricci-flat metric. Owing to Tian's theorem, the convergence of metrics on the line bundle $\mathcal{L}$ goes by the order of $\mathcal{O}(k^{-2})$. Then on $\mathcal{L}^k$, the use of algebraic metrics is expected to have an exponential convergence[2] (i.e. order of $\mathcal{O}(k^\nu)$ for any ν) [10] which we will not attempt to explain.

To summarise, we can iterate any initial $h^{\alpha\bar{\beta}}_{(0)}$ through the T-map infinite times to obtain a Ricci-flat metric. However, in practice, it was shown by [17] that there is no need to iterate more than 10 times for a good approximation owing to its fast convergence. Starting from $h^{\alpha\bar{\beta}}_{(0)}$, we have the sequence,

$$h_{(n+1)} = [T(h_{(n)})]^{-1} \tag{4.5}$$

that takes $h^{\alpha\bar{\beta}}$ to give us our desired metric in the limit of $n \to \infty$.

4.1.1 Error measures

To define what a good approximation is, let us introduce some error measures. Consider ourselves on a Calabi-Yau threefold. We define the "σ-measure" as a measure of how well the numerical metric satisfies the Monge-Ampére equation. Recall and adopt the notation from Chapter 3.4, the condition to satisfy the Monge-Ampére equation is $v_w =$ constant. Let us define,

$$\mathrm{Vol_K} = \int_X w \wedge w \wedge w, \qquad \mathrm{Vol_{CY}} = \int_X \Omega \wedge \bar{\Omega}. \tag{4.6}$$

By comparing the two top-forms, we can eliminate the need to compute v,

$$\frac{w \wedge w \wedge w}{\mathrm{Vol_K}} = \frac{\Omega \wedge \bar{\Omega}}{\mathrm{Vol_{CY}}}. \tag{4.7}$$

[2] It was shown the algorithm did not achieve exponential convergence. See Ch 4.3.

Denote w_k to be the Kähler form with respect to $g^{(k)}_{\alpha\bar{\beta}} = \partial_\alpha \partial_{\bar{\beta}} K_h$. If the metric is Ricci-flat, then the fractions $w_k^3/\operatorname{Vol}_{\mathrm{K}}$ and $\Omega\wedge\bar{\Omega}/\operatorname{Vol}_{\mathrm{CY}}$ equals to 1. We define,

$$\sigma_k \equiv \frac{1}{\operatorname{Vol}_{\mathrm{CY}}} \int_X \mathrm{dVol}_{\mathrm{CY}} \left| 1 - \frac{w_k^3/\operatorname{Vol}_{\mathrm{K}}}{\Omega \wedge \bar{\Omega}/\operatorname{Vol}_{\mathrm{CY}}} \right| \tag{4.8}$$

as the σ-measure. Clearly, $\sigma_k \sim 0$ indicates a good approximation to the Calabi-Yau metric. It was shown by [36, 14] that σ_k tends to 0 by the order of k^{-2}.

The σ-measure measures how well the metric solves the Monge-Ampére equation and has no direct relation to the Ricci scalar. We can define another measure, the "$\mathcal{R}$-measure", that measures the Ricci flatness via the Ricci scalar,

$$\mathcal{R} = \frac{\operatorname{Vol}_{\mathrm{K}}^{1/3}}{\operatorname{Vol}_{\mathrm{CY}}} \int_X \mathrm{dVol}_{\mathrm{K}} |R_{\mathrm{k}}|, \tag{4.9}$$

where R_{k} is the Ricci scalar of the balanced metric. The factors in front of the integral are included to eliminate scaling dependence on k. This quantity only vanishes if the balanced metric equals to the exact Calabi-Yau metric.

4.1.2 Implementation and Point sampling

Both the T-map and the σ-measure are involved in integrating over X. Due to the highly non-linear nature of (4.3), it is impossible to evaluate the integrals through analytic methods. This is why we turn to numerical methods. However, we face a computational challenge as integrating over the threefold (i.e. 6 real dimensions) is computationally expensive and inefficient with traditional numerical methods. This is often the biggest hurdle in applying the algorithm to more complicated geometries and in achieving better resolutions for the metrics. The common strategy to counter the problem is to use Monte Carlo methods in evaluating integrals, as Monte Carlo methods generally perform well in handling problems with high dimensionality.

Let us construct a measure on X, $\mathrm{d}\mu_\Omega$, such that,

$$\int_X f \mathrm{d}\mu_\Omega = \int_X f \Omega \wedge \bar{\Omega}. \tag{4.10}$$

A Monte Carlo integration is carried out by first sampling N_p points, p_i, uniformly according to the measure $\mathrm{d}\mu_\Omega$, then summing over them,

$$\int_X f \mathrm{d}\mu_\Omega = \int_X f \frac{\mathrm{d}\mu_\Omega}{\mathrm{d}A} \mathrm{d}A \approx \frac{1}{N_p} \sum_{i=1}^{N_p} f(p_i) w(p_i) \tag{4.11}$$

where $\mathrm{d}A$ is some density measure for the point sampling of x_i, and $w = \mathrm{d}\mu_\Omega / \mathrm{d}A$ serves as a weight. It will become clear later that $\mathrm{d}A$ is related to the induced Fubini-Study metric on X. Such a scheme allows us to avoid all the complications that come with the construction of coordinate patches.

There are numerous ways to sample points on a X, and we shall describe two of them here. The first step in both methods involves sampling points randomly on the projective space. Recall the isomorphism $\mathrm{S}^{2N+1}/\mathrm{U}(1) = \mathbb{CP}^N$. We can sample points on the projective space by sampling points randomly on the sphere, then we mod out the U(1) phase. A detailed description of this procedure is provided in [37]. The next step for the first method is to define "precision", that is to define a quantity to determine how well the generated point satisfies the defining polynomial of Q. We reject the point if it does not satisfy our required precision. This is called a rejection-type algorithm. It does not work efficiently for our case due to the high dimensionality nature of the Calabi-Yau.

The second method is an algorithm developed by [33] that shows how we can generate points on Q by intersecting lines with it. Consider a Calabi-Yau n-fold constructed as the zero locus of degree d homogeneous polynomial Q. We start by constructing a random line in $\mathbb{CP}^{n+1}$ through sampling a pair of points (a, b) randomly, where $a, b \in \mathbb{CP}^{n+1}$. A theorem by Bezout tells us there are d intersecting points between X and a line in $\mathbb{CP}^{n+1}$. Thus, by generating M lines on the projective space, we obtain $N_p = d \times M$ points on X. Explicitly, let us consider a line on $\mathbb{CP}^{n+1}$ written as $\lambda a + \rho b$ where λ and ρ are some complex variable. We then solve for λ and ρ that satisfies $Q(\lambda a + \rho b) = 0$ to obtain d-points $\lambda a + \rho b$ on Q. The major advantage of this setup is that the points generated by this method are uniformly distributed

with respect to the Fubini-Study metric on $\mathbb{CP}^{n+1}$. This is a result of the theorem of Shiffman and Zelditch, which allows us to write the density measure as the pullback of the volume form of the FS metric $\mathrm{d}A \sim i_p^*(w_{\mathrm{FS}}^3)$. See more in §3.2 of [33].

Having an algorithm to generate points on the manifold, it is crucial to ask how many points should we generate for a good approximation. There are three numbers that we should consider. The first is N_p, which is the number of random points needed to approximate the T-map integral with Monte Carlo integration. The second is N_g, which is the number of points used in obtaining the metric $g_{\alpha\bar{\beta}} = \partial_\alpha \partial_{\bar{\beta}} K_h$. The third is N_t, which is the number of points used in computing the error measure. An experiment carried out by [36] finds that N_p has to be larger than N_k^2, the number of parameters of the metric $h^{\alpha\bar{\beta}}$, for the balanced metric to converge properly. Later, the same authors [14] find that an ideal choice of points would satisfy,

$$N_p = 10N_k^2 + 50000. \tag{4.12}$$

For N_t, it was suggested by [17] that $N_t = 10000$ would be sufficient for checking approximations that have an error up to 1%.

The Fermat Quintic

Let us take the quintic as an example to illustrate how the polynomial basis can be constructed. Recall the defining polynomial of the quintic,

$$Q(z) = \sum_{i=1}^{5} (z_i)^5 = (z_1)^5 + (z_2)^5 + (z_3)^5 + (z_4)^5 + (z_5)^5 = 0 \subset \mathbb{CP}^4, \tag{4.13}$$

and it admits a nowhere vanishing holomorphic (3,0)-form,

$$\Omega = \left(\frac{\sum_{\mu=2}^{5} dz_2 \wedge ... \wedge z_\mu \wedge ... \wedge dz_5}{(\partial Q / \partial z_1)} \right) \Bigg|_{Q=0}. \tag{4.14}$$

We can construct the basis $\{s_\alpha\}$ as independent monomials of degree-k. There are N_k numbers of them, that is $N_k = \binom{5+k-1}{k}$. To see this, consider

$$
\begin{aligned}
&k=1,\ N_k=5 && \{s_\alpha\}=\{z_1,...,z_5\}\\
&k=2,\ N_k=15 && \{s_\alpha\}=\{z_1z_1,z_1z_2,\ldots,z_2z_2,z_2z_3,\ldots,z_3z_3,z_3z_4,\ldots,z_4z_5,z_5z_5\}\\
&k=3,\ N_k=35 && \{s_\alpha\}=\{z_iz_jz_k\},\ 1\leq i\leq j\leq k\leq 5
\end{aligned}
$$

From the defining polynomial (4.13), we can write $(z_1)^5=-\sum_{i=2}^5(z_i)^5$. Therefore on Q, the monomials are no longer independent and we have a reduced number of independent monomials for $k\geq 5$. Taking $k=5$ as an example, we could have $\{s_\alpha\}=\{(z_1)^5,(z_2)^5,(z_3)^5,(z_4)^5,(z_5)^5,...\}$. However, $(z_1)^5$ is actually the minus of the sum of the other 4 monomials, and thus $\{s_\alpha\}=\{(z_2)^5,(z_3)^5,(z_4)^5,(z_5)^5,...\}$.

Therefore, we have a refinement to N_k,

$$
N_k=\begin{cases}\binom{5+k-1}{k}, & 0<k\leq 4\\ \binom{5+k-1}{k}-\binom{k-1}{k-5}, & k\geq 5.\end{cases}
\tag{4.15}
$$

We can generalise the above to a Calabi-Yau embedded into $\mathbb{CP}^N$,

$$
N_k=\left\{\begin{matrix}\binom{N+k}{k}, & 0<k\leq N\\ \binom{N+k}{k}-\binom{k-1}{k-N+1}, & k\geq N.\end{matrix}\right\}\sim k^N \quad \text{for large } k.
\tag{4.16}
$$

For large k, we have $N_k^2\sim k^{2N}$ parameters for $h^{\alpha\bar{\beta}}$. This number also represents the dimension of the subspace of the Kähler class of Q defined by K_h. We can interpret this k^{2N} degrees of freedom as having k "Fourier modes" in every direction.

During points sampling, one can choose $z_i=1$ on the i-th patch of $\mathbb{CP}^4$, where $i=1,...,5$. There are two merits in doing so, the first is that it labels the patch we are on, while the second is it allows us to further eliminate another variable z_j within the patch via $Q=0$. Consider $z_1=1$, we can write $z_2^5=-(1+z_3^5+z_4^5+z_5^5)$ and thus we have only (z_3,z_4,z_5) as the independent coordinates on the patch. Then, we find $\Omega=(dz_3\wedge dz_4\wedge dz_5)/5z_2^4$, which can be used to obtain the $\Omega\wedge\bar{\Omega}$.

4.2 Energy Functional Approach

The problem with Donaldson's algorithm is that integrating over the Calabi-Yau manifold is a computationally challenging task. An alternative to Donaldson's algorithm is the energy functional approach advocated by Headrick and Nassar [15], where they have identified a set of "energy" functionals that has a minimum corresponding to the Ricci-flat metric. By minimising the Energy functional, we obtain the Ricci-flat metric, which is referred to as the "optimal" metric in the literature. The merit of this approach is that minimising a function is easier than solving the T-map integral in Donaldson's algorithm. This approach has three steps. The first two steps are to find the energy functionals and to find a way to represent the metric numerically. The final step is to minimise the functionals.

Let X be a n-dimensional Calabi-Yau manifold with a holomorphic volume form Ω and a Kähler form w. Recall the notation from Chapter 3.4, we have the volume form $\mu = (-i)^n \Omega \wedge \bar{\Omega}$, and the ratio $v_w = \det g_{i\bar{j}}/|\Omega_{1\ldots n}|^2$. Define the volumes,

$$V_M = \int_X \mu v_w, \qquad V_\mu = \int_X \mu \tag{4.17}$$

where V_M and V_μ is the volume with respect to the Kähler form and the volume form respectively. These are compatible with the one previously defined in (4.6). We have two functionals,

$$H_1[w] \equiv \int_X \mu (v_w - \frac{V_M}{V_\mu})^2 = \int_X \mu v_w^2 - \frac{V_M^2}{V_\mu}, \tag{4.18}$$

$$H_2[w] \equiv \int_X \mu g^{\bar{j}i} \partial_i \ln v_w \partial_{\bar{j}} \ln v_w = -\frac{1}{2} \int_X \mu R_w \tag{4.19}$$

where R_w is the Ricci scalar. Both of these functionals are non-negative and have only one critical point, which is a minimum that corresponds to the Ricci-flat metric. We can interpret the first functional as the standard deviation of v_w. In practice, one should only use H_1 during the minimisation process as the gradient in the Ricci scalar $R_w = -\nabla_w^2 \ln v_w$ from H_2 is difficult to obtain.

The second step is to represent the metric numerically. Similar to Donaldson's algorithm, the use of algebraic metrics is adopted, that is writing the Kähler potential in terms of a polynomial basis. By doing so, we restrict ourselves to Calabi-Yaus which are constructed as an algebraic variety. However, the energy functional approach takes another step, that is it uses the symmetry of the Calabi-Yau to reduce the dimensionality of the Kähler class constructed by the algebraic metrics.

Let us take the Fermat quintic as an example. It is well known that the quintic admits a $\mathbb{Z}_5 \times \mathbb{Z}_5$ symmetry group (see [38] for details), with generators

$$S : z_i \to \zeta^i x_i \quad \text{and} \quad T : z_i \to z_{i-1} \tag{4.20}$$

where z_i, $i = 1, ..., 5$, are the homogeneous coordinates of $\mathbb{CP}^4$, and ζ is a $(4+1)$-root of unity $e^{2\pi i n_i/(4+1)}$. We can interpret S as multiplying by a root of unity, and T as permutations of z_i. In addition, it admits a $z_i \to \bar{z}_i$ complex conjugate $\mathbb{Z}_2$ symmetry. Denoting Γ as the product of the three symmetry groups, we find the order of $\Gamma = 2(4+1)^4(4+1)! = 150000$, where 2 comes from the complex conjugation, $(4+1)!$ comes from the permutation, and $(4+1)^4$ comes from multiplying the root of unity to each z_i. The importance of these symmetry groups is that they require the Kähler potentials and its metrics to be invariant under them.

Instead of imposing the symmetry conditions on s_α, Headrick and Nassar go on to construct a new basis that is invariant under Γ and is independent of each other, $\mathcal{P}^l = c^l{}_{I\bar{J}} \bar{s}^{\bar{J}} s^I$, where $c^l{}_{I\bar{J}}$ is some coefficient that can be fixed numerically. Then they replaced $h_{\alpha\bar{\beta}}$ by h_l and rewrote the Kähler potential, $K_h = \frac{1}{k} \ln (h_l \mathcal{P}^l)$. The metric information is now encoded in h_l that has only one index. During the minimisation, the space of Kähler metrics is being scanned, which is varying the parameter h_l, and it picks out the algebraic metric that is closest to Ricci-flat. By exploiting the symmetry on the quintic, we reduce the dimensionality of the Kähler class and thus gain computational efficiency. The algebraic metric that minimises the energy functional is called "optimal".

We will not show how the minimisation is done explicitly. However, it is worth noting the Monte-Carlo method mentioned previously is adopted in evaluating the energy functionals. Furthermore, error measures defined in Chapter 4.1.1 also apply here.

4.3 Merits and Limitations

A worrying point for both methods is that each computation for the metric is fixed at a particular point on the moduli space. To elaborate, the basis holomorphic sections s_α implicitly fixes our complex structure, while the choice of line bundle $\mathcal{L}$ and thus the Kähler class $c_1(\mathcal{L})$ fixes our Kähler moduli. While it is still possible to study the moduli space, it is inefficient as one would need to rebuild the setup in every calculation. Another problem is that the Kähler forms on our Calabi-Yau X are constructed as the pullbacks of the Kähler forms on the projective spaces. This is obviously another limitation as we can only obtain a subspace of the Kähler class on X. Perhaps these are the drawbacks of adopting algebraic metrics.

On the contrary, the merit of using algebraic metrics is that it is easy to manipulate and keep the algorithm simple. Firstly, the polynomial basis is generally simple to construct and compute. Polynomials are also friendly to work with from a theoretical standpoint. Secondly, it bypasses the need to construct coordinate patches. Finally, we have, effectively, only one parameter to vary, that is the degree-k of the polynomial basis and thus is user friendly.

Consider the Donaldson algorithm. Despite its fast convergence, the computational cost rises exponentially with increasing k, resulting in a drastic drop in its efficiency. Taking $k = 8$ and $k = 12$ as an example, we have $N_8 \sim 4000$ and $N_{12} \sim 20000$ on the quintic, which implies the metric h having $\sim 16 \times 10^6$ and $\sim 4 \times 10^8$ numbers of parameters. From our previous discussion on the points required to generate a good approximation, we will need around 10^8 number of points for $k = 8$ case, which is a significantly large number to handle for a typical home-use PC. It was shown by

[17] that it takes 50 hours to complete the $k = 12$ case on the quintic, and predicted that it would take 35 years for $k = 20$. Bear in mind that any computation is fixed in a single point on the moduli, and thus 50 hours of computation is considered slow if we were to move through the moduli space.

The Donaldson algorithm approximates a balanced metric that converges to a Ricci-flat metric, instead of an actual Ricci-flat metric. Thus, there are two-fold error sources to our approximation, that is the statistical error from Monte Carlo integration and the error from the convergence to a Ricci-flat balanced metric. In contrast to the Donaldson algorithm, the energy functional minimisation directly approximates a Ricci-flat metric instead of an intermediate, such as the balanced metric. Therefore, we expect the energy functional approach to outperform the Donaldson algorithm in the same degree-k of the polynomial basis.

Let us include some reported values of the σ and $\mathcal{R}$ measures of the numerical Calabi-Yau metrics. From the energy functional approach [15], no $\mathcal{R}$-measures were computed. However, they have found $\sigma \simeq 0.17 \times 2.2^{-k}$ from the data of $k = 1$ to 10. Taking $k = 4, 6, 8$, it translates to $\sigma \simeq 0.00725, 0.00149, 0.00030$. For Donaldson Algorithm from [17], we have

$$k = 8, 10, 12 \;\Big|\; \sigma \simeq 0.04, 0.027, 0.02 \;\Big|\; \mathcal{R} \simeq 3.06, 2.13, 1.69.$$

Above σ-values agrees with the findings of [33], where $\sigma \simeq 3.1k^{-2} - 4.2k^{-3}$. Taking $k = 20$, we find $\sigma \simeq 0.00725$, which is the result for $k = 4$ for optimal metrics.

Notice that the balanced metric did not achieve an exponential convergence as expected from the use of algebraic metrics. It is clear that the optimal metrics are better than the balanced metrics by order of magnitudes. However, the major limitation of the algorithm is that it relies on the symmetries of the Calabi-Yau manifold. Unfortunately, most of the Calabi-Yaus of interest to string theory has little to no symmetries. This is a great limitation to the energy functional approach, as no symmetries imply the Kähler class which it scans over is big, resulting in low efficiency.

It appears that both aforementioned numerical methods face the problem of high computational time. Fortunately, techniques from machine learning can be used to mitigate this problem. For instance, neural networks can be applied to predict the output of the Donaldson algorithm for large values of k. It was found that machine learning techniques greatly increase the efficiency of the algorithm at the cost of little loss in the accuracy of the metric. [17] Moreover, the study of moduli dependence is made possible through the use of machine learning [16, 39].

5 Machine Learning

Machine learning is a rapidly evolving technology which is known for its excellence at approximating functions, classifying images and predicting sequential data. In the past few years, theoretical physicists began to borrow techniques from machine learning to study the string landscape [40, 41], AdS/CFT correspondence [42], bundle cohomology [43] and more. There are numerous attempts made to study Calabi-Yau metrics with machine learning [44, 39, 45, 16, 46, 47, 37, 48] and had led to fruitful results. The common feature seen among these works is the use of neural networks as a tool to approximate the Calabi-Yau metrics. In this chapter, we will review how neural networks approximate functions and discuss if the application of machine learning is necessary. We refer readers to [8, 49] for a physicists-oriented text on the application of machine learning to fundamental physics.

Before introducing neural networks, let us take a look at the general idea of what machine learning does and what we wish to achieve through it. Let us now refer to a neural network as a "machine". There are three common types of machine learning: unsupervised machine learning, supervised machine learning and reinforcement learning. For our purposes, we shall only focus on supervised machine learning. Considering its application, one typically starts by supplying the machine with some sample data, and "teaches" the machine what data it should produce. Through the learning process, the machine optimises its internal parameters to generate a "correct" output from a set of unseen data.

The whole process can be classified into four steps. The first step is *data acquisition*, where we acquire sample data with known "input" and "output". Let us call such sample data the training data. The second step is *learning*, where we feed our machine with the training data. The third step is *validating*, where we use a set

of validation data which was hidden from the machine to verify if the machine actually outputs the correct results. We call machine learning successful if the machine generates results that agree with the validation data. If machine learning is successful, we proceed to the final step called *predicting*, where we use our machine to predict results for data that has no known "output".

Let us take the Machine learning Donaldson algorithm to illustrate the above concretely. We first acquire a set of data $\mathcal{D}$ from the Donaldson algorithm for small value k. We split $\mathcal{D}$ into a training data set $\mathcal{T}$ and validation set $\mathcal{V}$, such that $\mathcal{D} = \mathcal{T} \cap \mathcal{V}$. We take $\mathcal{T}$ to train our "machine" to predict the output of the Donaldson algorithm. To examine if learning is successful, we cross-check its output with $\mathcal{V}$ by measuring how much percentage agreement they have with each other. We can also vary the size of $\mathcal{T}$, such as taking $\mathcal{T}$ to be 10%, 20%, etc. of $\mathcal{D}$ to see if the "machine" performs better. In general, the performance of the "machine" increases with the size of $\mathcal{T}$, but its improvement in performance diminishes as $\mathcal{T}$ continues to grow. After validation, we can apply our "machine" to predict the output of higher k-values of the Donaldson algorithm. The above procedure was adopted by [17], where they found the machine learning approach with curve fitting[1] is faster than the Donaldson algorithm by a factor of 50 times for the same level of accuracy on the quintic (i.e. accuracy achieved by the Donaldson algorithm for $k = 12$). With this significant improvement in efficiency, repeated computations with different complex structures and Kähler moduli are made possible within hours in contrast to the original 50 hours for a single computation.

A similar application of machine learning is carried out by [48], where they used "machine" to replace the minimisation procedure of the energy functional approach and thus gain efficiency. However, the obvious drawback of both methods is the need for a training dataset, which must be computed by the original algorithm. For

[1] A curve fitting technique is used to extrapolate for $g^{(k=15)}$ which serves as training data for the neural network to increase accuracy.

instance, if we were to consider a Calabi-Yau X with no symmetry, the method proposed by [48] would first require us to compute the metric of X via the energy functional minimisation algorithm to obtain a training dataset, which will be time-consuming. Furthermore, metrics obtained via the aforementioned methods are merely an approximation of what Donaldson or the energy functional algorithm would produce. Therefore, their accuracy will not be any better than the original algorithm. These are the limitations of direct supervised learning due to our ignorance of explicit Calabi-Yau metrics.

Can we use machine learning, not as a tool to improve the numerical methods, but as a tool to obtain the metric directly? The answer is yes, and there are currently a couple of open-sourced libraries, such as `CYJAX` [37], `cymetric` [16] and `MLGeometry` [45], made available for all physicists. Note that both `CYJAX` and `MLGeometry` adopt an algebraic Kähler potential ansatz. Furthermore, `CYJAX` was applied to study moduli-dependent metrics and SU(3) structure Calabi-Yau metrics [39], while `cymetric` was applied to study the moduli spaces of quintic and bicubic Calabi-Yau [16] and the complete intersection and Kreuzer-Skarke Calabi-Yau Manifolds [47].

Do they perform better than the Donaldson or the energy functional minimisation algorithm? It was reported by [37] that `CYJAX` achieves a σ-measure 4.4 times smaller than that of the Donaldson algorithm for $k = 6$ on the Dwork family quintic threefold. Authors of `MLGeometry` [45] have found their package performs better than the energy functional approach in manifolds with fewer symmetries. Finally, [16] reported that `cymetric` is capable of producing metrics of accuracy on par with $k = 20$ of the Donaldson algorithm with only a few hours on a laptop.

It was clear that machine learning techniques improve both the efficiency and accuracy of the metrics compared to that of traditional numerical methods. The magic of machine learning lies within the "machine", which is a neural network (NN) that learns to compute for a metric. Let us investigate how NN actually works.

5.1 Introduction to Neural Networks

Neural network, given by its name, tells us it mimics how a human brain behaves. A neural network generally consists of multiple layers of nodes which are interconnected by edges modelled by linear transformations. On each node, there is an activation function which is activated upon receiving an input or a signal. After processing the signal, the activation function outputs another signal which is relayed to its subsequent layer. In general, edges carry different weights, while nodes carry biases.

A neural network can be thought of as a general function approximator[2], which approximates functions $f : \mathbb{R}^n \to \mathbb{R}^m$. Suppose we wish to use a neural network to approximate the Calabi-Yau metric on the Dwork family quintic. How many input and output parameters do we need for the NN? For the input, we would need 5 complex coordinates and thus 10 real coordinate that specifies where we are on the quintic. We can also include a 5-dimensional array with only one non-trivial entry to specify which coordinate patch we are on (i.e. [1,0,0,0,0] specifies the 1-st patch). Finally, we would need 1 complex coordinate (2 real coordinates) to specify the parameter ψ of the quintic. Together, we have 17 inputs for the NN. For the output, the Calai-Yau metric is a hermitian matrix which has 3 real degrees of freedom from the diagonal and 3 complex degrees of freedom from the off-diagonal. Therefore, we have 9 output parameters for the NN. Thus, the neural network would be approximating a function $f : \mathbb{R}^{17} \to \mathbb{R}^9$, where we would need 17 input nodes and 9 output nodes. This is the NN setup of [16] to study the size and shape of the quintic.

Formally, a node is called a *neuron* which is a function $\sigma(\sum w_i x_i + b)$, where σ is its activation function, x_i is its argument, w_i is weight of edge and b is a bias. Typically, the range of the function is in $[0, 1] \subset \mathbb{R}$. Let us consider a simple section of a neural network shown in Figure 5.1 to show how a neuron works.

[2]It is often thought of as a highly nonlinear regressor. However, to avoid going into the concept of regression, we shall take the idea as NN can approximate any function we like.

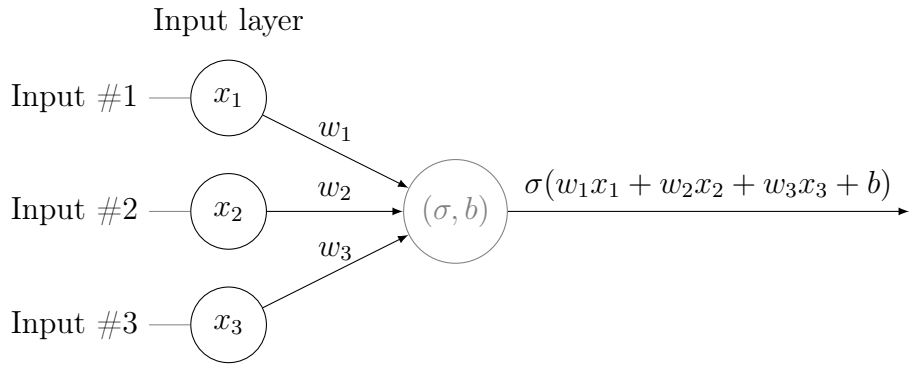

Figure 5.1: Three neurons with different edge weights connected to another neuron.

The figure shows a section of a NN with 3 input neurons connected to an intermediate neuron. We call the first layer of the network as *input layer*. Each "arrow" connecting the neurons is called an *edge* with a weight w_i. The intermediate neuron has an *activation function* σ and a *bias* b. Notice that both the weight and bias are assigned with a random value at the beginning and serve as the internal parameters of the NN. The NN relays the weighted input (i.e. $w_i x_i$) to the intermediate neuron and produces an output, $\sigma(w_1x_1 + w_2x_2 + w_3x_3 + b)$, which will be the "new" input for its subsequent connected neurons.

In Figure 5.2, we show a typical NN architecture which approximates a function $f : \mathbb{R}^3 \to \mathbb{R}^2$. We see every NN has an input and output layer. In between the two layers, there can be numerous layers of neurons which are called the hidden layers. Hidden layers are called hidden as the information relayed between them is never shown to us. There are no restrictions on the number of neurons in the hidden layers or the number of hidden layers. In fact, it is not even clear what configurations of the hidden layer would give the best-performing NN. We call the number of neurons in a layer the *width*, while the number of layers in a neural network the *depth*. Such a NN is commonly referred to as the "forward feeding NN", as we have only forward-propagating layers indicated by the arrows. If a NN has many hidden layers, then we call the NN *deep*, and it falls into the context of deep learning. If a NN has many nodes per layer, we call the NN *wide*.

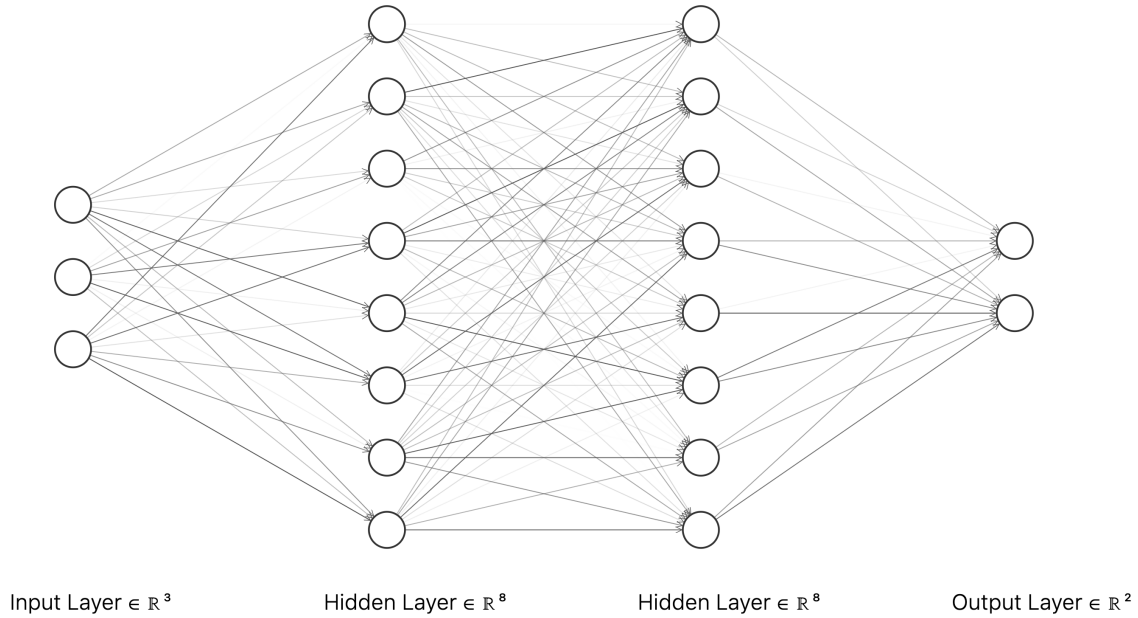

Figure 5.2: A typical NN architecture where the opacity of edge represents weight.

To formalise the above discussion, let us introduce some technical jargon in the context of machine learning. Suppose we have an *input vector* $\in \mathbb{R}^{n_0}$ where its elements are the input entries of a neural network. We call the elements of the vector *features*, and the corresponding (vector) space $\mathbb{R}^{n_0}$ the *feature space*. If we want the NN to produce values in $\mathbb{R}^{n_s}$, then we call the desired output values the *target values*.

Let us define n_i and $l_\mu^{(i)}$ be the width and the output of the μ-th neuron of the i-th layer respectively. Let us define $w_{\mu\nu}^{(i)}$ be the weight matrix of the i-th layer, where ν runs from 1 to n_{i-1} and μ runs from 1 to n_i. Notice that the ρ-th column of $w_{\mu\nu}^{(i)}$ encodes all the weights of the edges connected to the ρ-th neuron in the $(i-1)$-th layer. We then have,

$$z_\mu^{(i)} = \sum_{\nu=1}^{n_{i-1}} w_{\mu\nu}^{(i)} l_\nu^{(i-1)} + b_\mu^{(i)}, \qquad \mu = 1, 2, ..., n_i, \tag{5.1}$$

where $b_\mu^{(i)}$ is the bias on the μ-th neuron in the i-th layer, and $z_\mu^{(i)}$ is value that the activation function takes in the i-th layer.

The complexity of a neural network comes from its activation function, which is non-linear. We can pick different activation functions for different layers. However,

every neuron in the same layer has to have the same activation function. Applying the activation function on $z_\mu^{(i)}$, we get

$$l_\mu^{(i)} = \sigma^{(i)}(z_\mu^{(i)}). \tag{5.2}$$

Consider a NN with $(s+1)$ layers, where $i = 0$ denotes the input layer, and $i = s$ denotes the output layer. Now, we can write an expression that equates the output of the NN by substituting (5.2) into (5.1) recurrently,

$$f: \quad \mathbb{R}^{n_0} \to \mathbb{R}^{n_s}, \tag{5.3}$$

$$l_{\mu_s}^{(s)} = f(x) \tag{5.4}$$

$$= \sigma^{(s)}\Big(\sum_{\mu_{s-1}=1}^{n_s-1} w_{\mu_s\mu_{s-1}}^{(s)} \sigma^{(s-1)}(\dots \sigma^{(1)}(\sum_{\mu_0=1}^{n_0} w_{\mu_1\mu_0}^{(1)} l_{\mu_0}^{(0)} + b_{\mu_1}^{(1)})\dots) + b_{\mu_s}^{(s)}\Big), \tag{5.5}$$

where $x \in \mathbb{R}^{n_0}$, $l^{(s)} \in \mathbb{R}^{n_s}$ and $l_{\mu_s}^{(s)}$ is the μ_s-th entry of $l^{(s)}$.

Below are some common choices for the activation function,

$$\begin{array}{lll}
\text{Identity:} & f: \mathbb{R} \to \mathbb{R}, & f(x) = x \\
\text{Logistic sigmoid:} & f: \mathbb{R} \to (0,1), & f(x) = (1+e^{-x})^{-1} \\
\text{Tanh:} & f: \mathbb{R} \to (-1,1), & f(x) = \tanh(x) \\
\text{Leaky ReLU:} & f: \mathbb{R} \to \mathbb{R}, & f(x) = \begin{cases} x & x \geq 0 \\ -cx & x < 0, \end{cases} \\
\text{ReLU:} & f: \mathbb{R} \to \mathbb{R}, & f(x) = \begin{cases} x & x \geq 0 \\ 0 & x < 0. \end{cases}
\end{array}$$

There is currently no good explanation as to why some activation functions are better than others in some particular tasks (i.e. in regression or classification). Each activation function has its merits and drawbacks, and the best activation function for one's task is often found through trial and error.

One might wonder what is the role of the weights and the biases in the above setup. As we see the weights rescale the signal while the biases give an offset to the weighted

sum. Therefore, we can interpret that the weights are controlling the influences of input, while biases serve as the threshold for activation. Taking the ReLU as an example, if $w_i x_i$ is smaller than b (take b negative), then the resulting signal would be 0. Alternatively, adding a positive bias b can also help in activating the neuron. During the training process, these internal parameters (i.e. weights and biases) will be varied until they are "optimised", that is until the NN gives us the desired value. If we were to remove all the biases from the NN, then the resulting NN would not have as much freedom to tune for the best approximation. Note that removing all the biases from a small NN would greatly impact its performance in general.

5.2 Training the Neural Network

As mentioned previously, training the neural network amounts to tuning its internal parameters (i.e. weights and biases). In the context of supervised machine learning, the NN is trained to seek internal parameters that output values close to the given target values. A common technique used to carry out this task is called gradient descent. For us, we can train the NN by using this technique to minimise the σ-measure derived from the Monge-Ampére equation. Here, the σ-measure is the loss function of the NN. Let us adopt the notation in Chapter 5.1 on the discussion of a NN with $(s+1)$ layers.

The idea of gradient descent is to search for a minimum on the loss function by following the direction of steepest descent. Let us denote L as the loss function, and collectively denote the parameters of the μ-th neuron in the i-th layer by $\theta_\mu^{(i)}$. The gradient descent algorithm obtains a minimum by iterating through,

$$\theta_\mu^{(i)} \to \theta_\mu^{(i)} - \eta \frac{\partial L}{\partial \theta_\mu^{(i)}}, \tag{5.6}$$

where η is called the learning rate. We can interpret this map as sending $\theta_\mu^{(i)}$ down the steepest slope of L by a distance proportional to η.

To update the values of $\theta_\mu^{(i)}$, one needs the technique called backpropagation, which is essential in calculating all the gradients of L. Let us first rewrite the gradient on the i-th layer with the chain rule,

$$\frac{\partial L}{\partial \theta_\mu^{(i)}} = \frac{\partial L}{\partial z^{(i)}} \frac{\partial z^{(i)}}{\partial \theta_\mu^{(i)}} \tag{5.7}$$

where z is defined in (5.1). To illustrate the idea concretely, let us take L to be the mean square error function,

$$L = \frac{1}{n_s} \sum_{\mu=1}^{n_s} (y_\mu - l_\mu^{(s)})^2 \tag{5.8}$$

where y_μ is the target value. To simplify the notation, we introduce

$$\delta_\nu^{(s)} := \frac{\partial L}{\partial z_\nu^{(s)}}. \tag{5.9}$$

We can interpret $\delta^{(s)}$ as a measure of how much the output $l^{(s)}$ deviates from the target value. Let us compute this derivative on the output layer,

$$\frac{\partial L}{\partial z_\nu^{(s)}} = -\frac{2}{n_s}(y_\nu - \sigma^{(s)}(z_\nu^{(s)})) \frac{\partial \sigma^{(s)}(z_\nu^{(s)})}{\partial z_\nu^{(s)}} = -\frac{2}{n_s}(y_\nu - \sigma^{(s)}(z_\nu^{(s)}))\sigma'^{(s)}(z_\nu^{(s)}) \tag{5.10}$$

where we have used equation (5.2). We can proceed to $\delta_\nu^{(s-1)}$,

$$\delta_\nu^{(s-1)} = \frac{\partial L}{\partial z_\nu^{(s-1)}} = \frac{\partial L}{\partial z_\mu^{(s)}} \frac{\partial z_\mu^{(s)}}{\partial z_\nu^{(s-1)}} = \delta_\mu^{(s)} \frac{\partial z_\mu^{(s)}}{\partial z_\nu^{(s-1)}}. \tag{5.11}$$

From equation (5.1) and (5.2), we find,

$$\frac{\partial z_\mu^{(i+1)}}{\partial w_{\mu\nu}^{(i+1)}} = l_\nu^{(i)}, \quad \frac{\partial z_\mu^{(i+1)}}{\partial b_\mu^{(i+1)}} = 1, \tag{5.12}$$

$$\frac{\partial z_\mu^{(s)}}{\partial z_\nu^{(s-1)}} = \frac{\partial}{\partial z_\nu^{(s-1)}}(w_{\mu\nu}^{(s)} l_\nu^{(s-1)} + b_\mu^{(s)}) = w_{\mu\nu}^{(s)} \sigma'^{(s-1)}(z_\nu^{(s-1)}). \tag{5.13}$$

Notice that the summation sign is suppressed. Now substitute (5.13) into (5.11),

$$\delta_\nu^{(s-1)} = \sum_{\mu=1}^{n_s} (w_{\mu\nu}^{(s)} \delta_\mu^{(s)}) \sigma'^{(s-1)}(z_\nu^{(s-1)}). \tag{5.14}$$

We do this recurrently until we have exhausted the whole network. Essentially, we are propagating the information of $\delta^{(i)}$ backwards to obtain $\delta^{(i-1)}$ and thus yield the name backpropagation. We can generalise (5.14) to the i-th layer by replacing s

with i. Now, putting everything back into (5.7), we find

$$\frac{\partial L}{\partial w_{\mu\nu}^{(i)}} = \frac{\partial L}{\partial z_{\mu}^{(i)}} \frac{\partial z_{\mu}^{(i)}}{\partial w_{\mu\nu}^{(i)}} = \delta_{\mu}^{(i)} l_{\nu}^{(i-1)}, \quad \frac{\partial L}{\partial b_{\mu}^{(i)}} = \delta_{\mu}^{(i)}. \tag{5.15}$$

Thus, the weights and biases are updated by,

$$w_{\mu\nu}^{(i)} \to w_{\mu\nu}^{(i)} - \eta \delta_{\mu}^{(i)} l_{\nu}^{(i-1)}, \quad b_{\mu}^{(i)} \to b_{\mu}^{(i)} - \eta \delta_{\mu}^{(i)}. \tag{5.16}$$

One iteration of gradient descent concludes after updating all the internal parameters in all layers. This is repeated until we have reached a point where $\partial L / \partial \theta_{\mu}^{(i)} = 0$.

If the learning rate is too large, the algorithm might miss the minima or even climb up the slope of L. On the other extreme, a small learning rate might result in a long training time. Therefore, picking the right learning rate is crucial. Notice that the search will stop if it arrives at a critical point, that is point with a vanishing gradient. An immediate concern is if there exist many saddle points, what happens if the search gets stuck on them? Moreover, how can we tell apart a saddle point and a minima? Fortunately, there are numerous learning schemes and variants of gradient descent provided in Chapter 3 of [49] that help in choosing a good learning rate and overcoming problems associated with saddle points.

Another concern of the training is how one splits the sample data. Notice that apart from the weights and biases, we have variables such as the number of hidden layers, the number of neurons per hidden layer and learning size, which are fixed during the design of the neural network. All of these parameters are called hyperparameters. We cannot modify them like the weights and biases during the training process. Therefore, it would be beneficial to split the data into a training set, a validation set and a testing set. The training set, undergoing gradient descent, would give us the optimised weights and biases. We then use the validation set to see how the NN performs if we vary the hyperparameters. Finally, the testing set would be used to evaluate the performance of the NN after we have found the best hyperparameters. One of the widely used hyperparameter tuning methods is called grid

search, where one trains the NN for a set of possible combinations of the preselected hyperparameters to search for the best-performing configuration.

5.3 Application to Calabi Yau metrics

Having the basic idea of how neural networks "learn", let us take a look at how it was applied to solve a Calabi-Yau metric. Let us restrict ourselves to the open-sourced libraries `CYJAX`, `MLGeometry` and `cymetric`. As mentioned earlier, both `CYJAX` and `MLGeometry` adopt an algebraic Kähler potential ansatz. Despite it automatically ensuring a Kähler metric, it restricts us to a subspace of the Kähler class of the Calabi-Yau. On the other hand, `cymetric` solves this problem by introducing two loss functions, which we shall explain later. Furthermore, `cymetric` is the only library, out of the three mentioned here, that has the capability to study complete intersection and Kreuzer-Skarke Calabi-Yau manifolds. Restricted by the length of this dissertation, let us only study how `cymetric` gives a CY metric.

The size and shape of a Calabi-Yau is studied in [16, 47] with `cymetric`. In particular, let us see how the volume of the Calabi-Yau X is computed. Let us denote w_{CY} as the Ricci-flat Kähler form, and w_{FS} as the Kähler form induced by the Fubini-Study metric from the ambient space (i.e. $\mathbb{CP}^4$ for the Fermat quintic). Similar to equation (4.6), we define two volume forms,

$$\mathrm{dVol}_{\mathrm{CY}} = \frac{1}{3!} w_{\mathrm{CY}}^3, \quad \mathrm{dVol}_{\mathrm{FS}} = \frac{1}{3!} w_{\mathrm{FS}}^3. \tag{5.17}$$

We find the volumes by integrating the volume form,

$$\mathrm{Vol}_{\mathrm{CY}} = \int_X \mathrm{dVol}_{\mathrm{CY}} = \int_X d^6x \sqrt{g_{\mathrm{CY}}}, \quad \mathrm{Vol}_{\mathrm{FS}} = \int_X \mathrm{dVol}_{\mathrm{FS}} = \int_X d^6x \sqrt{g_{\mathrm{FS}}} \tag{5.18}$$

where g denotes the determinant of metric. To obtain the volumes numerically, one needs the Monte-Carlo integration. Notice that if both w_{CY} and w_{FS} are in the same Kähler class, we find their volume coincides.

In `cymetric`, points on the Calabi-Yau are sampled by the intersecting lines method

described in Chapter 4.1.2. Thus, the sampled points are distributed according to the measure $\mathrm{d}A$, which can be used to perform Monte-Carlo (MC) integration,

$$\int_X \mathrm{dVol}_{\mathrm{CY}} f = \int_X \frac{\mathrm{dVol}_{\mathrm{CY}}}{\mathrm{d}A} f = \frac{1}{N} \sum_i w_i f|_{p_i}, \quad w_i = \left. \frac{\mathrm{dVol}_{\mathrm{CY}}}{\mathrm{d}A} \right|_{p_i}. \tag{5.19}$$

Finally, we can compute the volume by performing MC integration on (5.18).

As discussed at the beginning of Chapter 5.1, the neural network of `cymetric` takes 10 (5 complex coordinates) + 5 (array specifying the patch) + 2 (complex coordinate for ψ) = 17 inputs. Remarkably, the package offers five options in how the Ricci-flat metric, g_{CY} is predicted:

Name of mode	Output
Free	$g_{\mathrm{CY}} = g_{\mathrm{NN}}$
Additive	$g_{\mathrm{CY}} = g_{\mathrm{FS}} + g_{\mathrm{NN}}$
Multiplicative, element-wise	$g_{\mathrm{CY}} = g_{\mathrm{FS}} + g_{\mathrm{FS}} \odot g_{\mathrm{NN}}$
Multiplicative	$g_{\mathrm{CY}} = g_{\mathrm{FS}} + g_{\mathrm{FS}} \cdot g_{\mathrm{NN}}$
ϕ-model	$g_{\mathrm{CY}} = g_{\mathrm{FS}} + \partial\bar{\partial}\phi$

Here, we denote the output of the NN for the first four options as g_{NN} and denote the output for the last option as ϕ. Clearly, g_{NN} has 9 real-components and ϕ is just a scalar. In theory, different choices have their own merits, but it was shown some perform better in the quintic experiment.

The NN architecture of `cymetric` is relatively simple. It has an input layer with 17 neurons, an output layer with 9 neurons, three hidden layers each with 64 neurons and GELU (Gaussian Error Linear Unit) activation functions. An Adam (Adaptive Moment Estimation) optimizer is used in training.

There are five loss functions to ensure the output satisfies the Monge-Ampére equation. We write the total loss function,

$$\mathcal{L} = \alpha_1 \mathcal{L}_{\mathrm{MA}} + \alpha_2 \mathcal{L}_{\mathrm{d}w} + \alpha_3 \mathcal{L}_{\mathrm{transition}} + \alpha_4 \mathcal{L}_{\mathrm{Ricci}} + \alpha_5 \mathcal{L}_{\mathrm{Vol\text{-}K}} \tag{5.20}$$

where α_i are hyperparameters, $\mathcal{L}_{\mathrm{MA}}$ is called Monge-Ampére loss, $\mathcal{L}_{\mathrm{Ricci}}$ is called

Ricci loss, $\mathcal{L}_{dw}$ is called Kähler loss, $\mathcal{L}_{\text{transition}}$ is called transition loss and $\mathcal{L}_{\text{Vol-K}}$ is called the Kähler class loss. The individual loss functions are defined as follows,

$$\mathcal{L}_{\text{MA}} = \left\| 1 - \frac{1}{v} \frac{\det g_{\text{CY}}}{\Omega \wedge \bar{\Omega}} \right\|_n , \quad w \wedge w \wedge w = v\Omega \wedge \bar{\Omega} \tag{5.21}$$

$$\mathcal{L}_{\text{Ricci}} = \left\| \partial\bar{\partial} \ln \det g_{\text{CY}} \right\|_n \tag{5.22}$$

$$\mathcal{L}_{dw} = \sum_{ijk} \left\| \text{Re } c_{ijk} \right\|_n + \left\| \text{Im } c_{ijk} \right\|_n , \quad c_{ijk} = \partial_k g_{i\bar{j}} - \partial_i g_{k\bar{j}} \tag{5.23}$$

$$\mathcal{L}_{\text{transition}} = \frac{1}{d} \sum_{\mathcal{U},\mathcal{V}} \left\| g^{\mathcal{V}}_{\text{CY}} - T_{\mathcal{U}\mathcal{V}} \cdot g^{\mathcal{U}}_{\text{CY}} \cdot (T_{\mathcal{U}\mathcal{V}})^\dagger \right\|_n \tag{5.24}$$

$$\mathcal{L}_{\text{Vol-K}} = \left\| \int \det g_{\text{FS}} - \int \det g_{\text{CY}} \right\|_n . \tag{5.25}$$

Here, $\|x\|_n$ denotes the L_n norms of x. By default, $n = 1$ for all loss functions, except for $\mathcal{L}_{dw}$ which has $n = 2$. In equation (5.24), $\mathcal{U}$ and $\mathcal{V}$ denotes the patches on X, and $(T_{\mathcal{U}\mathcal{V}})^\nu_\mu = \partial x^\nu / \partial y^\mu$ are the transition functions on the chart overlapping region, where x and y are the local coordinates on chart $\mathcal{U}$ and $\mathcal{V}$ respectively.

We see $\mathcal{L}_{\text{MA}}$ is similar to the σ-measure, $\mathcal{L}_{\text{Ricci}}$ is actually the Ricci-scalar, $\mathcal{L}_{dw}$ is the Kähler condition, $\mathcal{L}_{\text{transition}}$ is the agreement of g_{CY} on the overlapping region, and $\mathcal{L}_{\text{Vol-K}}$ measures if w_{CY} and w_{FS} are in the same Kähler class. Using these five loss functions, we can ensure the output g_{CY} to be Ricci-flat, Kähler and consistent on the overlapping chart region. This resolves the need for an algebraic Kähler potential ansatz at the cost of two loss functions, $\mathcal{L}_{\text{transition}}$ and $\mathcal{L}_{dw}$.

5.4 Merits and Limitations

The experiment [47] is carried out on the quintic and bi-cubic Calabi-Yau. Let us focus on the result reported on the quintic. All five of the output modes of the package were used to solve for a Ricci-flat metric on the quintic threefold. It was shown that machine learning is successful (i.e. loss function continues to decrease) for all of the output options. Particularly, the multiplicative, $g_{\text{CY}} = g_{\text{FS}}(\mathbb{I} + g_{\text{NN}})$, and ϕ-model, $g_{\text{CY}} = g_{\text{FS}} + \partial\bar{\partial}\phi$, were found to outperform the other options.

For the multiplicative model, the NN is learning how to correct the induced Fubini-Study metric to be a Ricci-flat metric. The merit of this approach is that the FS metric is already complex (i.e. has smooth transitions between patches) and Kähler, (i.e. $\mathcal{L}_{\text{transition}}$ and $\mathcal{L}_{\text{d}w}$ are already minimised to start with) and thus alleviates the need to optimise all five loss functions. An immediate drawback is that it might not work well if the Calabi-Yau metric is not connected to the Fubini-Study metric. In other words, g_{NN} is large. For the ϕ-model, the NN is seeking a Ricci-flat Kähler potential. The metric g_{CY} is by construction Kähler, which allows us to ignore both $\mathcal{L}_{\text{transition}}$ and $\mathcal{L}_{\text{d}w}$. However, it would require us to compute two additional derivatives which raises the computational cost.

It was reported by [47] that the ϕ-model, trained with 100 epochs[3] within an hour of runtime on a laptop, achieves a $\sigma = 0.0086$ and $\mathcal{R} = 0.076$. The result is on par with $k = 20$ balanced metrics and $k = 4$ optimal metrics. Note that it was extrapolated by [17] that $k = 20$ would take 35 years to finish the balanced metric approximation.

This shows the application of machine learning indeed has reached its original goal, which is to shorten the runtime of the calculation. In addition, the machine learning approach produces metrics via minimising the Ricci scalar and the deviation from the Monge-Ampére equation. It does not require us to specify for a Kähler class, and we can study the moduli dependence by specifying the point on the moduli during the training process. This is something both the Donaldson algorithm and the Energy functional minimisation algorithm lack. Another merit of the machine learning technique is that it allows us to study Ricci-flat but non-Kähler metrics on manifolds of special structure. This can be done simply by adjusting our loss functions. It was studied by [39], where they showed the NN is capable of producing non-Kähler SU(3) structure metrics.

[3]Having the NN trained on the training data once is called one epoch.

Despite the machine learning approach failed to produce metrics with precision on par with large value k optimal metrics, it is evident that it allows us to study a wider range of Calabi-Yau manifolds and their moduli spaces at ease compared to that of conventional numerical algorithms. Another drawback of the approach is that it is difficult to predict the neural network's performance and to obtain a statistical error on the approximation. This is due to its highly non-linear nature. Lots of current work is still in the exploratory stage, and it involves lots of trial and error. However, there are many fantastic machine learning libraries, for instance, TensorFlow and PyTorch, available for us to implement and optimise our neural networks. As machine learning continues to evolve, one can expect future technologies to increase the accuracy of metrics, shorten the runtime, and eventually compute physical observables like the Yukawa couplings.

Before concluding this chapter, it is useful to give some examples of how numerical metrics were applied in physics. In [47], numerical metrics solved by `cymetric` were used to obtain a Hermitian Yang-Mills connection with an error $\sim 3\%$ on the bicubic manifold. In [50], the moduli-dependence of the massive KK modes and the swampland distance conjecture is studied with the application of optimal metrics. In [12], the Hermitian Yang-Mills connection on quartic K3 and quintic threefold is obtained by the use of balanced metrics.

6 Conclusion

In this dissertation, we gave an introduction to complex geometry and motivated the study of Calabi-Yau manifolds in the context of superstring theory. We reviewed the idea of dimensional compactification and briefly studied the notion of moduli spaces and its relation to string theory.

If one wishes to study the low energy effective field theory of a superstring theory on the Calabi-Yau manifold, especially the physical observables, the knowledge of the Calabi-Yau metric is indispensable. However, there are no known analytic expressions for the Ricci-flat metric, which motivates the study of numerical Calabi-Yau metrics. We reviewed two of the most common numerical algorithm that uses algebraic metrics to approximate the Ricci-flat metric. They are called the Donaldson algorithm and the energy functional minimisation algorithm. The former approximates the Calabi-Yau metric by a balanced metric, which converges to a Ricci-flat metric under iterations through a T-map; while the latter approximates the Calabi-Yau metric by an optimal metric, which corresponds to a minimum of some Energy functionals. It was found that the optimal metrics can achieve very high accuracy in a short runtime, while balanced metrics need a relatively longer time to reach the same accuracy as the optimal metrics. However, the energy functional approach is limited by the symmetry of the Calabi-Yau, making it less efficient in Calabi-Yaus which is of interest to string theory.

In the final section, we reviewed the basics of machine learning, and how it was applied to approximate for Calabi-Yau metrics. As discussed, machine learning techniques allow us to study a wider range of Calabi-Yaus and the moduli-dependence of the metrics. It is evident that machine learning brings benefits to physicists, and we hope it sheds light to uncharted regions in the study of Calabi-Yau manifolds.

Bibliography

[1] M. R. Douglas. "Calabi-Yau metrics and string compactification". In: (Mar. 2015). arXiv: 1503.02899.

[2] P. Candelas et al. "Vacuum configurations for superstrings". In: *Nucl. Phys. B* 258 (1985), pp. 46–74.

[3] E. Calabi. "The space of Kähler metrics". In: *Proceedings of the International Congress of Mathematicians, Amsterdam* 2 (1954), pp. 206–207.

[4] Shing-Tung Yau. "On the ricci curvature of a compact kähler manifold and the complex monge-ampére equation, I". In: *Commun. Pure Appl. Math.* 31.3 (1978), pp. 339–411.

[5] G. Tian and S. T. Yau. "Three dimensional algebraic manifolds with $c_1 = 0$ and $\chi = -6$". In: *Conf. Proc. C* 8607214 (1986), pp. 543–559.

[6] P. Candelas, C. A. Lutken, and R. Schimmrigk. "Complete Intersection Calabi-Yau Manifolds. 2. Three Generation Manifolds". In: *Nucl. Phys. B* 306 (1988), p. 113.

[7] M. Kreuzer and H. Skarke. *Calabi-Yau data*. URL: http://hep.itp.tuwien.ac.at/~kreuzer/CY/ (visited on 07/26/2023).

[8] Yang-Hui He. *The Calabi–Yau Landscape: From Geometry, to Physics, to Machine Learning*. Lecture Notes in Mathematics. May 2021. arXiv: 1812.02893 [hep-th].

[9] M. Headrick and T. Wiseman. "Numerical Ricci-flat metrics on K3". In: (June 2005). arXiv: hep-th/0506129.

[10] S. K. Donaldson. "Some numerical results in complex differential geometry". In: (2005). arXiv: math/0512625 [math.DG].

[11] Michael R Douglas et al. "Numerical solution to the hermitian Yang-Mills equation on the Fermat quintic". In: *Journal of High Energy Physics* 2007.12 (Dec. 2007), pp. 083–083. arXiv: hep-th/0606261.

[12] Lara B. Anderson et al. "Numerical Hermitian Yang-Mills connections and vector bundle stability in heterotic theories". In: *Journal of High Energy Physics* (June 2010). arXiv: 1004.4399.

[13] Lara B. Anderson, Volker Braun, and Burt A. Ovrut. "Numerical Hermitian Yang-Mills connections and Kähler cone substructure". In: *Journal of High Energy Physics* 2012.1 (Jan. 2012). arXiv: 1103.3041 [hep-th].

[14] Volker Braun et al. "Eigenvalues and Eigenfunctions of the Scalar Laplace Operator on Calabi-Yau Manifolds". In: *JHEP* 07 (2008), p. 120. arXiv: 0805.3689 [hep-th].

[15] M. Headrick and A. Nassar. "Energy functionals for Calabi-Yau metrics". In: (Aug. 2009). arXiv: 0908.2635.

[16] M. Larfors et al. "Learning Size and Shape of Calabi-Yau Spaces". In: (Nov. 2021). arXiv: 2111.01436.

[17] A. Ashmore, Y. H. He, and B. Ovrut. "Machine learning Calabi-Yau metrics". In: (Oct. 2019). arXiv: 1910.08605.

[18] M. Nakahara. *Geometry, topology and physics*. 2003.

[19] C. J. Isham. *Modern differential geometry for physicists*. 1999.

[20] V. Bouchard. *Lectures on complex geometry, Calabi-Yau manifolds and toric geometry*. 2007. arXiv: hep-th/0702063 [hep-th].

[21] P. Candelas. "Lectures on Complex Manifolds". In: *1987 Spring School on Superstrings (Trieste)* 1 (1987), pp. 1–88.

[22] S. Yau. "Calabi-Yau manifold". In: *Scholarpedia* 4.8 (2009). revision #170091. DOI: 10.4249/scholarpedia.6524.

[23] X. d. l. Ossa. *Calabi–Yau Manifolds and Mirror Symmetry*. Lecture notes for Oxford graduates, during HT 2010.

[24] Brian R. Greene. "String theory on Calabi-Yau manifolds". In: *Theoretical Advanced Study Institute in Elementary Particle Physics (TASI 96): Fields, Strings, and Duality*. June 1996, pp. 543–726. arXiv: hep-th/9702155.

[25] K Hori et al. *Mirror symmetry*. American Mathematical Society, 2003.

[26] Kim A. Frøyshov. *Projective spaces*. URL: https://www.uio.no/studier/emner/matnat/math/MAT4520/v21/notes/proj.pdf.

[27] R.C. Gunning and H. Rossi. *Analytic Functions of Several Complex Variables*. Printice Hall, Englewood Cliffs N.J., 1965.

[28] Michael R. Douglas. "Compactification of superstring theory". In: (2005). arXiv: hep-th/0508034 [hep-th].

[29] Michael B. Green, John H. Schwarz, and Edward Witten. *Superstring Theory: 25th Anniversary Edition*. Vol. 2. Cambridge Monographs on Mathematical Physics. Cambridge University Press, 2012. DOI: 10.1017/CBO9781139248570.

[30] F. Quevedo. *2015 Part III Lectures on Extra Dimensions*. DAMTP.

[31] Jiakang Bao et al. *Lectures on the Calabi-Yau Landscape*. 2020. arXiv: 2001.01212 [hep-th].

[32] D. Joyce. "Compact Manifolds with Special Holonomy". In: Oxford Mathematical Monographs. Oxford University Press, 2000.

[33] M. R. Douglas et al. "Numerical Calabi-Yau metrics". In: *J. Math. Phys.* 49 (2008). arXiv: hep-th/0612075.

[34] M. R. Douglas. *strategy*. URL: https://people.brandeis.edu/~headrick/Mathematica/strategy.pdf (visited on 07/20/2023).

[35] G. Tian. "On a set of polarized Kähler metrics on algebraic manifolds". In: *Journal of Differential Geometry* 32.1 (July 1990), pp. 99–130.

[36] V. Braun et al. "Calabi-Yau Metrics for Quotients and Complete Intersections". In: (Dec. 2007). arXiv: 0712.3563.

[37] Mathis Gerdes and Sven Krippendorf. "CYJAX: A package for Calabi-Yau metrics with JAX". In: *Mach. Learn. Sci. Tech.* 4.2 (2023), p. 025031. arXiv: 2211.12520 [hep-th].

[38] Philip Candelas and Challenger Mishra. "Highly Symmetric Quintic Quotients". In: (Apr. 2018). arXiv: 1709.01081.

[39] L. B. Anderson et al. "Moduli-dependent Calabi-Yau and SU(3)-structure metrics from Machine Learning". In: (Dec. 2020). arXiv: 2012.04656.

[40] Yang-Hui He. "Deep-Learning the Landscape". In: (June 2017). arXiv: 1706.02714 [hep-th].

[41] Yang-Hui He. "Machine-learning the string landscape". In: *Phys. Lett. B* 774 (2017), pp. 564–568. DOI: 10.1016/j.physletb.2017.10.024.

[42] K. Hashimoto et al. "Deep learning and the AdS/CFT correspondence". In: *Physical Review D* 98.4 (Aug. 2018). arXiv: 1802.08313 [hep-th].

[43] Callum R. Brodie et al. "Machine Learning Line Bundle Cohomology". In: *Fortsch. Phys.* 68.1 (2020). DOI: 10.1002/prop.201900087. arXiv: 1906.08730 [hep-th].

[44] V. Jejjala, D. K. M. Pena, and C. Mishra. "Neural Network Approximations for Calabi-Yau Metrics". In: (Dec. 2020). arXiv: 2012.15821.

[45] M. R. Douglas, S. Lakshminarasimhan, and Yidi Qi. "Numerical Calabi-Yau metrics from holomorphic networks". In: (Dec. 2020). arXiv: 2012.04797.

[46] Per Berglund et al. "Machine Learned Calabi-Yau Metrics and Curvature". In: (Nov. 2022). arXiv: 2211.09801 [hep-th].

[47] Magdalena Larfors et al. "Numerical metrics for complete intersection and Kreuzer–Skarke Calabi–Yau manifolds". In: *Mach. Learn. Sci. Tech.* 3.3 (2022). arXiv: 2205.13408 [hep-th].

[48] A. Ashmore et al. "Calabi-Yau Metrics, Energy Functionals and Machine-Learning". In: (Dec. 2021). arXiv: 2112.10872.

[49] Fabian Ruehle. "Data science applications to string theory". In: *Phys. Rep.* 839 (2020), pp. 1–117. DOI: 10.1016/j.physrep.2019.09.005.

[50] Anthony Ashmore and Fabian Ruehle. "Moduli-dependent KK towers and the swampland distance conjecture on the quintic Calabi-Yau manifold". In: *Phys. Rev. D* 103.10 (2021). arXiv: 2103.07472 [hep-th].